THE REPUBLIC OF TURKEY
BAHÇEŞEHİR UNIVERSITY

STUDY OF THE SCATTERING BASED LOSSES IN PASSIVE OPTICAL NETWORKS

Master's Thesis

GÜRKAN KAYA

İSTANBUL, 2015

THE REPUBLIC OF TURKEY
BAHÇEŞEHİR UNIVERSITY

THE GRADUATE SCHOOL OF NATURAL AND APPLIED SCIENCES COMPUTER ENGINEERING

STUDY OF THE SCATTERING BASED LOSSES IN PASSIVE OPTICAL NETWORKS

Master's Thesis

GÜRKAN KAYA

Supervisor: Assoc. Prof. SARPER ÖZHARAR

İSTANBUL, 2015

THE REPUBLIC OF TURKEY
BAHCESEHİR UNIVERSITY

THE GRADUATE SCHOOL OF NATURAL AND APPLIED SCIENCES

COMPUTER ENGINEERING

Title of Thesis: Study of the Scattering Based Losses in Passive Optical Networks
Name/Last Name of the Student: Gürkan Kaya
Date of Thesis Defense: May 11, 2015

The thesis has been approved by the Graduate School of Natural and Applied Sciences.

Assoc. Prof. Nafız ARICA
Graduate School Director

This is to certify that we have read this thesis and that we find it fully adequate in scope, quality and content, as a thesis for the degree of Master of Science.

Asst. Prof. Dr. Tarkan AYDIN
Program Coordinator

Examining Committee Members:	Signature
Thesis Supervisor Assoc. Prof. Sarper ÖZHARAR	_____
Member Asst. Prof. Tarkan AYDIN	_____
Member Assoc. Prof. Ömer ÇAKIROĞLU	_____

ACKNOWLEDGEMENTS

First of all I want to appreciate to my advisors Asst. Prof Sarper ÖZHARAR for all of their interest, support, idea, and auxiliary contributions for my thesis.

I also acknowledge my thesis committee members for their time.

Finally, special thanks my family, for their supports, and encouragements.

İSTANBUL, 2015 Gürkan KAYA

ABSTRACT

STUDY OF THE SCATTERING BASED LOSSES IN PASSIVE OPTICAL NETWORKS

Gürkan Kaya

Computer Engineering

Thesis Advisor: Assoc. Prof. Sarper ÖZHARAR

May 2015, 88 Pages

In recent years, rapid development of wireless data transmission has required that researchers and engineers who study data transmission and network topology, should focus on controlling the increased data traffic and dealing with the related challenges. Both increased number of users in data communications and the need of applications with higher capacity due to widely used internet, require broader bandwidth. Since such increase in data traffic service providers should enhance service quality provided for end users in parallel with such growth.

Optical fiber has become one of the essential elements of communication systems in recent years because of its high capacity for transferring the light at different wavelengths and having high performance together with large bandwidth in data transmission thanks to high carrier frequency of light. Especially large bandwidth of optical fiber has enabled a great number of users communicating on the same fiber cable simultaneously and resulted in a relief for traffic on the lines by providing high performance in data communication.

In data communication, long distance Passive Optical Networks will be crucial for optical fiber access networks in the future in terms of increasing bandwidth and reducing unit line cost.

During transmission throughout the optical fiber, a reduction in signal power occurs due to scattering mechanisms such as Rayleigh scattering resulting from inhomogeneity of fiber material and interaction with molecular models (Raman scattering) or acoustic waves resulting from thermal effects (Brillouin scattering).

In this thesis study, use of Passive Optical Network (PON) in data communication networks was discussed and several loss mechanisms are investigated. The main aim was to understand the signal reduction mechanisms so that some solutions can be offered as a future work.

Keywords: Passive Optical Networks (PON), WDM-PON, TDM-PON, PON links Scattering Induced Signal Attenuation, PON links.

ÖZET

PON LİNKLERDE SAÇILMA KAYNAKLI MEYDANA GELEN SİNYAL ZAYIFLAMALARININ ARAŞTIRILMASI

Gürkan Kaya

Bilgisayar Mühendisliği
Tez Danışmanı: Doç. Dr. SARPER ÖZHARAR

Mayıs 2015, 88 Sayfa

Son yıllarda, kablosuz veri iletiminde yaşanan hızlı büyüme, veri iletimi ve ağ topolojileri konularında çalışan araştırmacıların ve mühendislerin artan veri trafiğini kontrol etme ve bu zorluğun üstesinden gelme konularında yoğun olarak çalışmalarını gerekli hale getirmiştir. Gerek veri haberleşmesindeki kullanıcı sayısı artışı, gerekse internet kullanımının giderek yaygınlaşmasına paralel olarak kullanıcıların daha yüksek kapasite isteyen uygulamalara olan yönelimleri, daha yüksek bant genişliklerine gereklilik göstermiştir. Veri trafiğindeki bu artmaya bağlı olarak servis sağlayıcıların son kullanıcılara vereceği hizmetin kalitesini de bu gelişmeye paralel olarak arttırması gerekmektedir.

Optik fiberlerin, ışık taşımadaki yüksek kapasiteleri ve dolayısıyla ışığın modülasyonu ile veri iletimindeki yüksek verimlilikleri ve büyük bant genişliğine sahip olmaları nedeniyle, son yıllarda haberleşme sistemlerinin önemli elemanlarından biri olmuştur. Özellikle yüksek bant genişlikleri optik fiberlerin haberleşme sistemlerinde aynı anda çok sayıda kullanıcının aynı hattan haberleşmesine olanak sağlamış ve veri trafiğinin yüksek verimlilikte kullanılmasını da sağlayarak hat trafiğinin rahatlamasına neden olmuştur.

Veri haberleşmesinde, uzun erişim mesafeli Pasif Optik Ağlı linkler, geleceğin optik fiberli erişim ağları ve haberleşme sistemleri için bant genişliğini arttırmak açısından ve birim hat maliyetlerini azaltmak için çok önemlidirler.

İletim esnasında optik fiber boyunca, gerek fiber malzeme yapısındaki inhomojenlikten kaynaklanan Rayleigh saçılması ve fiber içerisinde ilerleyen optik sinyalin ortamda oluşan moleküler modlarla (Raman saçılması) veya termal etkilerle ortaya çıkan akustik dalgalar ile etkileşmesi (Brillouin saçılması) sonucu meydana gelen saçılma mekanizmaları nedeniyle, sinyalde bir zayıflama meydana gelmektedir.

Bu tez çalışmasında, veri haberleşmesinde ağ kullanımında, Pasif Optik Ağların (PON) kullanımına yer verilmiş ve farklı kayıp mekanizmaları incelenmiştir. Ana amaç sinyal azalma mekanizmalarının anlaşılması ve böylece gelecekteki çalışmalar için bazı çözümlerin sunulmasıdır.

Anahtar Kelimeler: Pasif Optik Ağlar (PON), WDM-PON, TDM-PON, PON Linklerde Saçılma Nedenli Sinyal Zayıflaması, PON Linkler.

TABLE OF CONTENTS

FIGURES

ABBREVIATIONS

ACF : Auto Correlation Function
AOM : Acousto-optic Modulator
ASE : Amplified Spontaneous Emission
AWG : Indexed Wave Guide Grille
BER : Bit Error Rate
BG : Bragg Grating
BOCDA : Brillouin Optical Correlation Domain Analysis
BOTDA : Brillouin Optical Time Domain Analysis
BOTDR : Brillouin Optical Time Domain Reflectometer
BPF : Band Pass Filter
CBS : Coherent Brillouin Sensor
CD : Coherent Detection
CLS : Centralized Light Source
CO : Central Office
CRN : Coherent Rayleigh Noise
CS : Current Source
CW : Continuous Wave
CWDM : Coarse Wavelength Division Multiplexing
DCA : Digital Communication Analyzer
DD : Direct Detect
DFB : Distributed Feedback Laser
DPMZ : Double-Pass Mach-Zehnder
DSP : Digital Signal Processing
EDFA : Erbium Doped Fiber Amplifier
ELO : Electrical Local Oscillator
EOM : Electro-optic modulator
ER : Extinguishing Rate
ESA : Electrical Spectrum Analyzer
FEC : Forward Error Correction
FPLA : Fabry-Perot Laser Amplifier
FTTB : Fiber-to-the-Building
FTTC : Fiber-to-the-Cabinet
FTTH : Fiber-to-the-Home
HCF : High Frequency Cut
HDTV : High Definition Television
FUT : Fiber Under Test
FWM : Four-Wave Mixing
IF : Medium Frequency

I/O	:	Input/Output
ISI	:	Intersymbol Interference
LEAF	:	Wide Domain Fiber
LFC	:	Low Frequency Cut
LO	:	Local Oscillator
LPF	:	Low Pass Filter
MD	:	Modulation Depth
MI	:	Stability of Modulation
MZM	:	Mach-Zehnder Modulator
NRZ	:	Non-return to Zero
OBPF	:	Optical Band Pass Filter
OEO	:	Optical-Electrical-Optical
OFC	:	Optical Fiber Communication Conference
ONU	:	Optical Network Unit
OSA	:	Optical Spectrum Analyzer
OSNR	:	Optical Signal to Noise Ratio
OSP	:	Optical Signal Processing
OTDR	:	Optical Time Domain Reflectometer
PBS	:	Polarization Beam Splitter
PM	:	Phase Modulator
PON	:	Passive Optical Network
PSD	:	Power Spectral Density
RB	:	Rayleigh Scattering
RF	:	Radio Frequency
RSOA	:	Reflective Semiconductor Optical Amplifier
RZ	:	Return to Zero
SBS	:	Stimulated Brillouin Scattering
SCM	:	Modulated Sub-carrier
SMF	:	Single-Mode Fiber
SPM	:	Self-Phase Modulation
TDM	:	Time Division Multiplexing
VOA	:	Variable Optical Attenuator
WDM	:	Wavelength Division Multiplexing
XGM	:	Cross-Gain Modulation

CHARTS

SYMBOLS

Acoustic frequency : fa

Acoustic velocity : v_a

Acoustic wave length : λ_a

Anti-Stokes frequency : v_{as}

ASE noise : I_{ASE} λ_{AS}

Anti-Stokes signal wavelength : λ_{as}

Attenuation : α

Average number of signal components above or processed data : N

Boltzmann constant : k

Bose-Einstein coefficient : $\wp$

Brillouin backscattered power : P_b

Brillouin frequency shift : v_b

Brillouin gain constant : g_b

Brillouin scattering coefficient : α_B

Brillouin scattering wavelength : λ_{bs}

Calculated by measuring the temperature variation of Raman : ΔT_R

Capture fraction : S

Change in power Raman : ΔP_R

Change in wavelength : $\Delta\lambda$

Compressible isothermal equilibrium : β_T

Core refractive index : n_{core}

Differential attenuation coefficient (Neper) : $\Delta\alpha p$

EDFA belonging to the input signal power : P_s

Effective core area : A_{eff}

Electric field : E

Equivalent bandwidth : B_{eq}

Fiber attenuation coefficient : α_{dB}

Fiber length : L

$w = (2\pi f)$

Frequency ( ) : w

Grating signal wavelength : λ_g

Group refractive index of the fiber core : n_{gr}

Group velocity : v_g

Impact, thermal origin and source of the FET : j

Impulse noise : i_{impact}

Modulation instability gain constant : G

Noise amplifier : $i_{amplifier}$
Operation wavelength : λ
Optical noise figure : F
Peak power laser : Po
Perceived average power of the anti-stokes (Watt) : $\overline{P}_{AS}$
Perceived average stokes power (Watt) : $\overline{P}_S$
Photon energy : $\hbar\omega_o$

Pulse width : W
Rayleigh scattering coefficient : α_R
Speed of light in space : c
The dispersion parameter : D
Planck's constant : h
Raman gain constant : gr
The measured Brillouin frequency shift : Δv
The pump and anti-Stokes Raman frequency difference : Δvr
Power exchange : ΔP
Temperature change : ΔT
Structural parameters : χ
The effective length : L_{eff}
Walk-off length : L_w
The probe signal : P_s
The pump signal : P_p
Power of injected into the signal fiber : P_o
Photo elastic constant : p
Wavelength : λ
The wavelength of the pump signal : λ_p
Stokes signal wavelength : λ_s λ_S
Responses of discrete signals stokes and anti-Stokes : h_s h_{AS}
Refractive index : n
Silica concentration : ρ
Pump frequency : v_o
Stokes frequency : v_s
Pump frequency : v_p
The spatial range : Δz
Respectively absolute temperature (ºK) and fictive temperature : T T_f
The laser pulse duration : τ
The number of wave wavelength separation between the Raman and pump : v_R
Refractive index Cases : n_{clad}
The cut-off wavelength fiber : λ_c
Temperature coefficient : C_t

Thermal noise current feedback resistor : R_f

Optical signal-to-noise ratio : SNR_0

Signal-to-noise power ratio : SNR_e

Spontaneous emission factor : n_{sp}

Saturation voltage : V_{sat}

Thermal noise : $i_{thermal}$

Thermal signal : i_{signal}

1. INTRODUCTION

Communication of huge number of subscribers over the same line, rapid increase of the use of internet, and users' tendency to the applications which require higher capacity caused the bandwidth needs to increase in communication networks.

These limitations in bandwidth are tried to be overcome with widespread use of increasing component varieties of optical fibers and unit bandwidth costs are reduced.

In line with researches conducted and results drawn in recent years by utilizing passive optical networks (PON) and splitters at several locations can be fed with a single fiber by utilizing passive optical Networks (PON) and splitters. One of the major advantages of passive optical networks is transmission of high capacity data to very long distances without the need of additional electric power and in this way it facilitates data transmission.

However, in communication networks where the optical fibers are used, there can be weakening in signals between transmitter and receiver in modulation and demodulation process and as well as based on transmission environment characteristics. Particularly when transmission is done via light in fiber optics, light can be scattered and reflected backwards. This scattering is a combination of Rayleigh scattering, which is generated by the fiber's density inhomogeneity, Raman scattering and Brillouin scattering, which are generated by molecular and volumetric vibrations respectively [1].

In PON links, Rayleigh scattering, Brillouin scattering and Raman scattering reduce the power of the light signal, which is injected into the fiber, due to non-linear effects, resulting in less optical power at the receiver side of the power.

1.1 GOAL OF THE THESIS

In recent years, distributed Raman fiber amplifiers (DRFA), amplifiers which are widely used for PON links, have become the focus of attention for researchers. Both the easiness of realization electronically and having more widespread area of usage economically as compared to Brillouin amplifiers have led to a shift in studies to this direction.

In this thesis study, the use of Passive Optical Network (PON) in data communication networks was discussed and several loss mechanisms are investigated. The main aim was to understand the signal reduction mechanisms so that some solutions can be offered as a future work.

1.2 OUTLINE OF THE THESIS

In this thesis, a general view of the passive optic networks are given. Their importance, properties, advantages and disadvantages are discussed.
In the following part, different scattering mechanisms and their effects are explained in detail.

In this study, a 1 Km. long PON link was used in order to find Raman intensity profile in reverse scattered signal. Some simulation conditions between OLT and ONU have been determined, thus, change in Raman intensity of reverse scattered signal was calculated as functions of temperature and time in accordance with simulation results of Matlab. Based on possible influences of temperature parameters on both between OLTs and ONUs and on splitter connection points on PON links for such points in addition to Raman intensity changes in Brillouin intensity resulting from temperature were also simulated.

2. CURRENT STATE OF OPTICAL NETWORKS

2.1 INTRODUCTION

In line with rapid developments in computer technology high bandwidth needs of service providers who serve for long distances, have increased rapidly for the last 40 years [2].

While transistor costs went down by half, and computation speed per unit of time doubled at every 18 – 24 months the cost of sending every bit of data per distance decreased by half and number of bits sent per unit of time has doubled in every 9 months [3]. In contrast to semiconductor technology, the rapid increase in this capacity not only planned technological developments but also may have had support from developments such as erbium fiber amplifiers, waveguide gratings and planar lightwave circuits [4].

Nowadays, high-bandwidth internet backbone is required along with data transmission in communication networks and due to voice and video design become more widespread which require high-bandwidth and thereby increase in bits per second and new applications come into our life. Developing fiber optical technology offers us this high capacity; however, transforming all communication systems into fiber optical infrastructure should be well considered when transformation costs are taken into account.

Initially, installation cost of fibers was the basic parameter in the construction and start-up of communication systems, in the later process intermediate connection elements which are used in optical networks and energy requirements of these elements and after care services have been accepted as important factors. From this perspective, carrying studies for passive optical network developing projects, and providing sustainability to these studies have become more appropriate.

In communication sector, first developments were on the double-stranded copper wires. At first these types of wires were used but they were insufficient to meet the needs of the system and they were replaced by fiber optical cables. With the help of light spectrum optical fiber lines transmits data between transmitter and the receiver.

Having done transmission with light in fiber optics and having light at 100s of terahertz ($10^{14} – 10^{15}$ Hz) frequencies range have made it possible to be used in high-bandwidth transmissions.

With developments in WDM technology data transfers at long distance links for gigabits per second (Gb/s) were possible. However, recent developments in high definition video, especially inventions in user-based high definition videos, have become strong and growing demand for "last mile" bi-directional bandwidth studies. "Last mile" term refers to connection between last user and first link on the net. This link is totally 50 km of line, 10 km of that is within the city and communication service is conducted electrically. That is to say, it is just the opposite of typical long distance backbone links in which communication is done optically.

Passive Optical Networks (PON) aim to carry high quantity of data for long distances with the help of fiber optic cables [5]. In passive optical network structures and systems, systems are named and classified based on where fiber optical cable reaches. This concept is called as "Fiber to the X" (FTTX). The letter "X" at the end indicates the type of the end point. Thereby, names such as FTTH, FTTP, FTTC, FTTB, are used in optical networks. For instance, letter "B" stands for "Building", "C" for "Cabinet", "P" for "Premises" and "H" for "Home" as the end point of the fiber line.

Countries in the world pay utmost attention to mobile and fixed bandwidth infrastructure. Furnishing fiber optical infrastructure to houses is rapidly taking place in countries like South Korea and Japan, which are pioneers in this field, also in USA and many other European countries such as Germany. Figure 2.1 indicates broadband subscribers by country over the world. FTTH, Fiber-to-the-Home systems are widely used by countries nowadays.

Figure 2.1: Broadband subscriber percentage by country

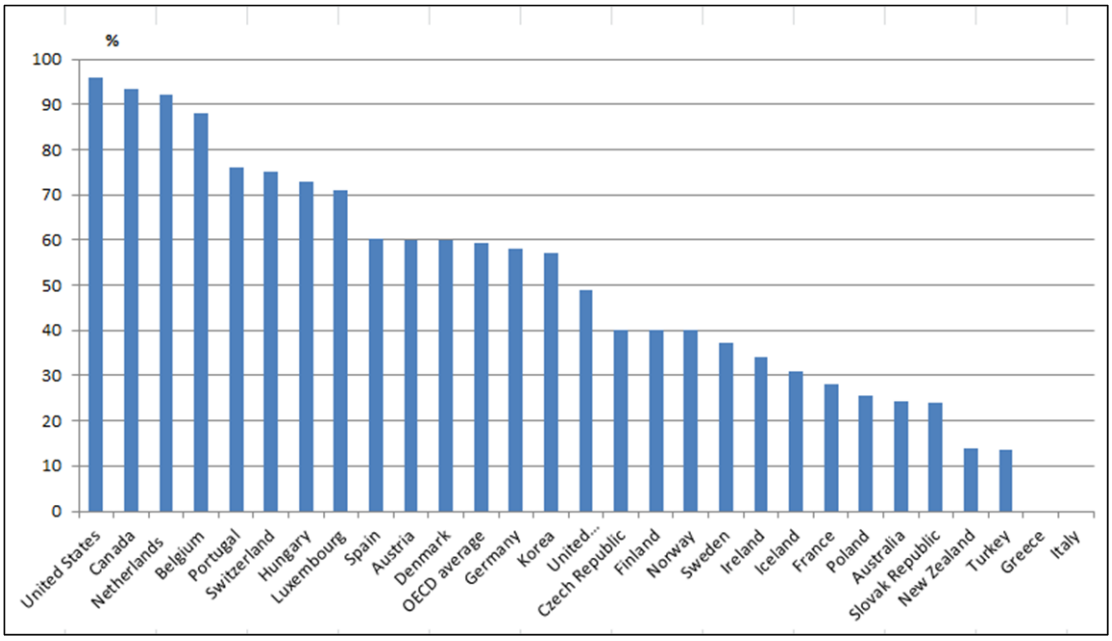

Source: http://www.oecd.org/sti/broadband/oecdbroadbandportal.htm (05.01.2015)

2.2 PASSIVE OPTICAL NETWORKS (PON)

PON architecture, which is developed by the end of 1980s, was first used in telecommunication systems. It has continuously been developed due to the broadband needs from those years on.

One of the most significant developments was the foundation of Full Service Access Network (FSAN) community. The most crucial contribution of FSAN was creation of an economic indicator schedule over the world, and development of low cost and standardized systems.

This system was based on PON and DSL. Later FSAN worked on specific working groups. Most importantly OAN (optical access network) group, they developed standards for systems with the name of International Telecommunication Union Standard Sector.

A PON system is comprised of OLT (optical line terminal), ONU (optical network unit), optical splitter which provides information (data) communication between the fiber optical cables which connects them to each other. In the system, data sent from OLT to ONU with the help of splitter and thereby communication is completed.

Ensuring that ONUs are not receiving distributed information which do not belong to them is one of the most crucial issue. Moreover, clashes of information should be prevented because information coming from all ONUs will be sent to OLT by utilizing single fiber optical cable after the splitter.

High transmission capacity of affective optical fiber communication lines are used in each stage in networks. Particularly fiber optic technology which is used in large-scale (metro Ethernet) networks are started to be used for serving the end-user in order to meet the need for higher capacity and to overcome the bandwidth limitation.

Replacing copper lines with fiber lines is costly for network operators although optical transmission is very fast. However when the cost-benefit analysis is done, it is necessary that he benefits and gains of the system should be more than the cost.

The most crucial advantages of passive optical networks are high-bandwidth high flexibility and relatively having lower-cost as compared to other systems. Figure 2.2 shows a simplified structure of a passive optical network [6].

Figure 2.2: Basic passive optical networks components

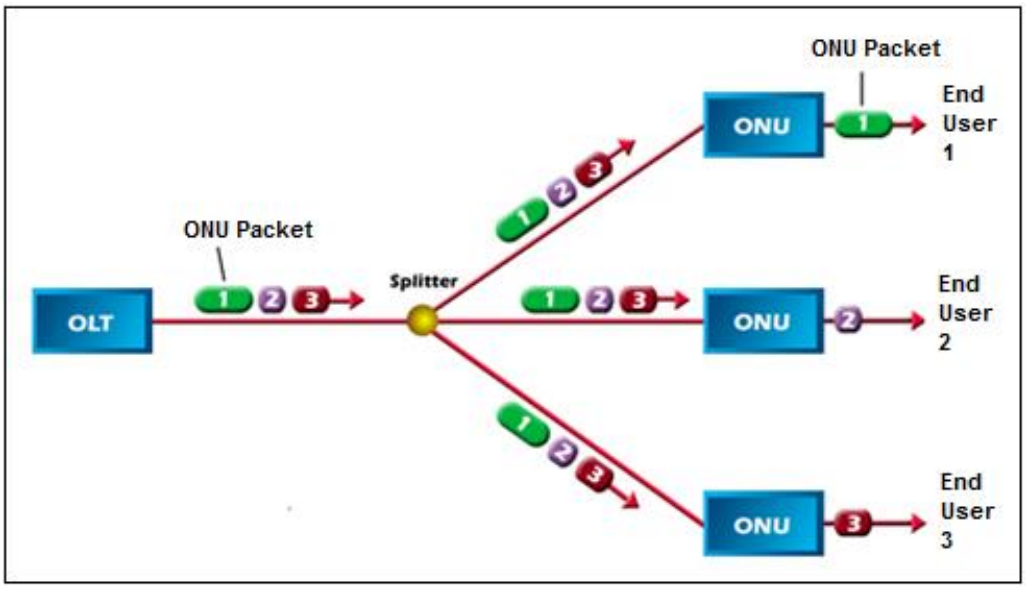

Source: http://www.gta.ufrj.br/ensino/eel879/trabalhos_vf_2008_2/rafael_ribeiro/E-PON.html (11.01.2015)

As it is indicated in Figure 2.2, a basic PON structure is composed of optical line terminal (OLT), optical network units (ONU), and passive splitters which distribute the information flow to ONUs and fiber optical cables which combines these devices to each other.

In the case where both links (both for transmitter and receiver parties) use the same wavelength in receiving data at OLT side, high-power effects become more important. Bit error rate (BER) measurements can be carried out at different transmission rates by using different techniques. Therefore, reducing or minimizing backward-scattering effects on the signal at the receiver side becomes possible.

In PON systems, data transmission from ONUs to OLT is done in the form of burst, and from OLT to ONUs is done though straight publication.

ONUs process the optical data received by them. Since ONUs receive all of the information (data) including the ones which do not belong to them, services to be developed ought to provide privacy of outbound packets. In other words, multi-access

systems needed to be used in order to prevent transmitted data clashes on the line because data which is transmitted from all ONUs to OLT will be in a position to use single fiber line.

Today, in the standardized PON structures TDMA (Time Division Multiple Access) method is used. Another multiple-access method, on which many research is done, called wavelength division multiple-access (WDMA).

Numerous studies in the literature target to increase the number of user and quantity of transmission by utilizing WDMA method alone, or TDMA and WDMA together in PON systems. WDM systems increase the number of reachable user as well as the cost of devices [7].

First PON standard which is published by ITU-T as standard of G.983 is APON-BPON [7]. It proposed to use ATM (Asynchronous Transfer Mode) mechanism for data transmission. It uses first named as APON since it was using packet transmission method based on ATM.

Then, in order to indicate that standard developed afterwards is not dependent on ATM packet transfer the name of BPON is used. It provides data transmission over maximum 20 km's and at 622 Mb/s downward and at 155 Mb/s upward. It predicts to use single mode fibers. Maximum split ratio of optical splitter is determined as 1:32.

BPON systems use TDMA method in order to provide multiple access. In G983.3 standard, a special region on optical spectrum was arranged for video services. Wavelength division multiplexing (WDM) method is used in order to help APON service with video service to work independently at provider and user side.

Distribution in network from a service provider in PON systems is shown in Figure 2.3.

Figure 2.3: Distribution of service provider

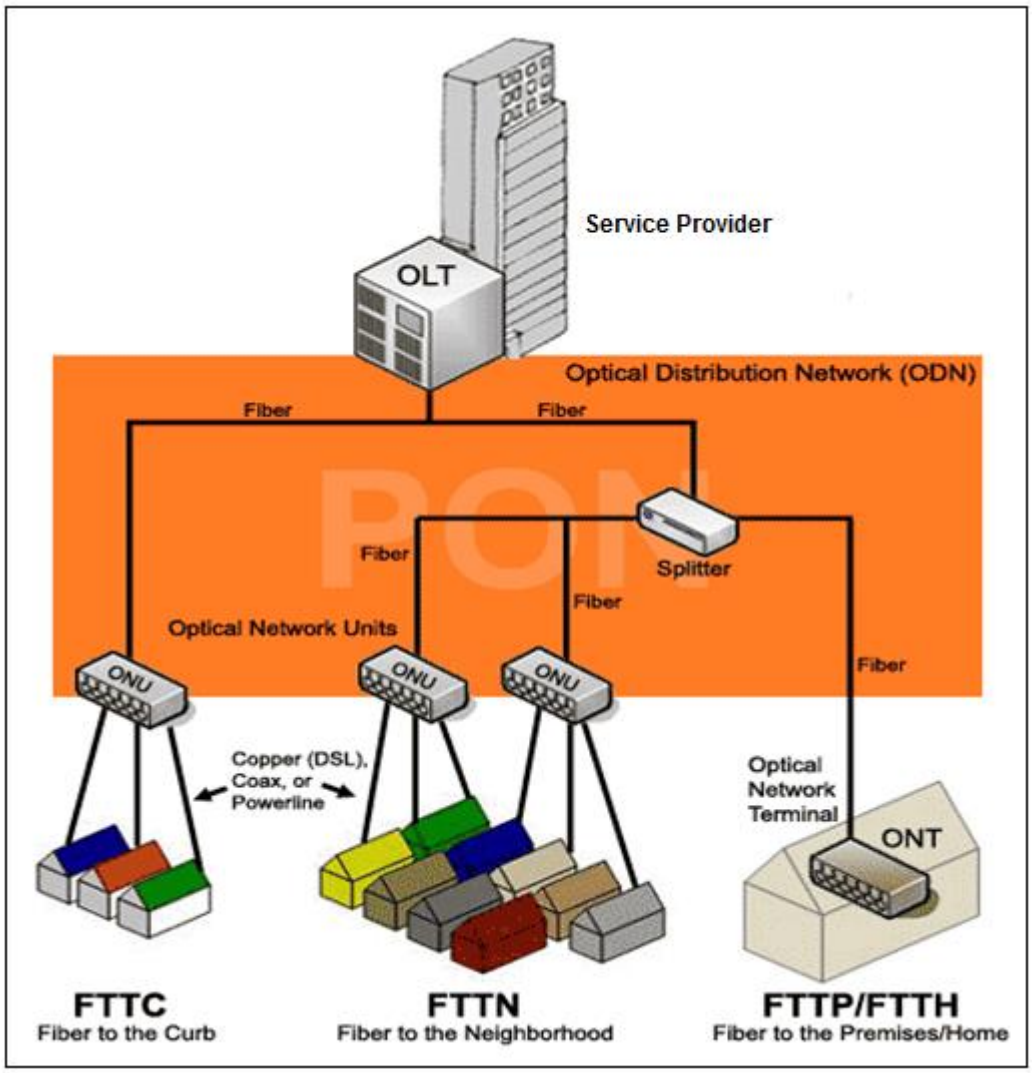

Source: http://ftth.blogsky.com/1391/06/30/post-3/ (14.01.2015)

GPON (Gigabit Passive Optical Network) is developed under ITU-T G.984. It proposes data transmission at 2.488 Gb/s for downward direction and at 1.244Gb/s for upward direction. Split ratio in optical splitters is 1:64 and it supports 1:128 standard for further applications as well.

Transportation of IP traffic in transmission network by means of dividing it into ATM cells brings additional load to the system. For this reason, instead of ATM cells used in BPON, frames of 125 μs are used. Within these frames, Ethernet, ATM or classic TDM

packages can be transported. With the help of this capsule mechanism, GPON has the opportunity to work with only Ethernet or only with ATM mode.

Although physical and transport layers are well defined in GPON, upper layers are not defined yet. Different line protection structures by multiplexing optical access networks fibers structures by multiplexing optical access network fibers are also defined in GPON standards in case of malfunctions in lines. Usage of this protection was left to service provider firm.

Usage of protection structure requires identification of some OAM (Operation, Administration, and Maintenance) frames.

Since the downward data transmission in passive optical networks is in the form of general publication, the required security measures are defined in the standard in order to prevent the access of other users to the private data.

EPON (Ethernet Passive Optical Network) standard was developed by the group IEEE 802.3ah EFM (Ethernet in the First Mile). The main difference of it from ATM PON systems is the usage of Ethernet packages of varying lengths instead of fixed ATM cells for data transmission.

EPON systems use fixed-length frames for downward and upward data transmissions. Each frame is composed of time slots which belong to different ONUs.

Ethernet packets are transported within these time slots undividedly. If an Ethernet packet does not fit to existing time slot dimensionally, it goes to next time slot.

Same with ATM PON, EPON uses 1.5μm wavelength band for downstream and 1.3μm wavelength band for upstream transmission. GEPON standard was developed in which symmetrical 1.25Gbps transmission was made possible for both directions.

Under IEEE802.3av, 10G-EPON standard was developed which made 10Gbps downflow and 1 Gbps upflow possible. FSAN (Full Service Access Network) NGA (Next Generation Access) group is trying to develop new generation optical access network standard over the GPON standard [9].

Many architectural and technological developments (such as use of WDM, 10Gbps transmission, optical amplifiers, etc.) have been examined for new generation access standard. This standard which will be developed in the future should be compatible with GPON and GEPON systems which are currently in use.

Numerous studies have been carried out in the world in order to increase the capacity, distance and amount of users in PON systems. These studies are mainly dealing with methods to decrease the amount of intermediate node electronic components and modifying the network into a simpler structure. PON standards used currently are working within 20km distance at 16 (BPON), 32 (EPON), 64 (GPON) split ratios.

In order PON systems to serve more users, systems are being designed which will have more splitting capacity.

There is need for optical amplifiers in order to increase split ratio because increase in split ratio in passive splitters will result in decrease in optical signal power. Besides, there is a need of optical amplifiers in order to eliminate decline in signal power for data transmitted within long distances on the fiber line between local variation points and central office.

Various technologies have been developed in order to meet the needs of power for increasing the split ratio and the distance: these are GPON expansion box, semiconductor optical amplifier, praseodymium/thulium fiber amplifiers, and transponders [10].

With the use of EDFA establishment of passive network systems with 10Gbps transmission speeds was seemed possible.

2.2.1 Time-Division Multiplexing PON

TDM is the one of the best known methods of PON architecture. This technique aims each user to be served at specific time periods.

Each user is entitled to use his/her entire bandwidth within the allotted time. In order to read more than one user at the same time in the system passive optical splitter is used.

Fiber line coming from central office serves "N" number of subscribers as it is going to be split by 1:N. OLT prevents data clash which will be sent to "N" number of user. It communicates with ONU for data transmission at user side.

As a useful feature in the times when some ONUs need to send so much data, time allotted to other ONUs will be transferred to other ONUs when there are not that much data in other ONUs. It is called as DBA (Dynamic Bandwidth Allocation). There are many DBA algorithms that allow this process.

Even though DBA algorithms increase the effectiveness of PON, algorithm control is not easy because user's “wants and needs” are not always same. As the need for bandwidth rises, transfer to QoS (Quality of Service) can be done. For instance, allocating additional buffer memory to users when are in the queue for transmitting (sending) data. However, QoS is not suitable for every architecture [11] [12].

PON systems, used widely today, allow downward data transmission and use TDM for separating upward directional data. The structure of a TDM PON was shown in Figure 2.4 [13].

It ignores other data, in other words it does not do any transaction with them. For an upstream data there is a different wavelength, it is used together with combination of wavelength division multiplexing filters.

The most important advantage of TDM PON is the low cost of fiber optical transmitter and receiver and possibility of decreasing fiber costs by dividing it to sub-subscribers.

Figure 2.4: Schematic representation of TDM-PON. In the representation, "n" number of ONUs on the same fiber.

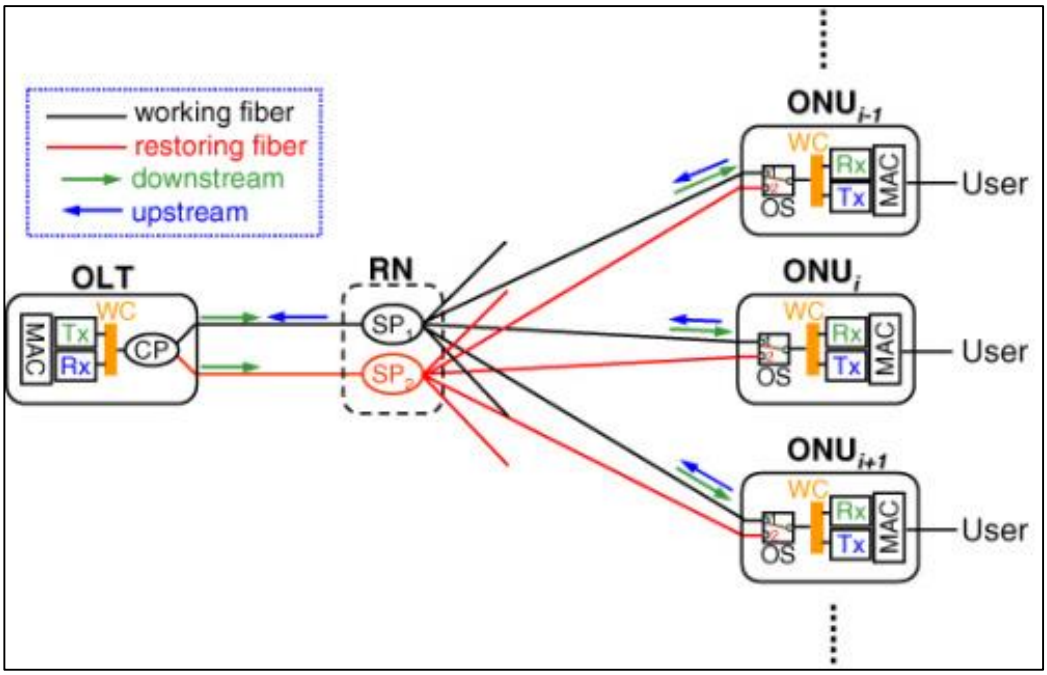

Source: https://www.osapublishing.org/oe/fulltext.cfm?uri=oe-16-7-4494 (14.01.2015)

Higher bandwidth needs are met by increasing the transmitter line speed in TDM-PONs.

2.2.2 Wavelength Division Multiplexing PON (WDM-PON)

Wavelength division multiplexing (WDM) PONs are alternative to time division multiplexing PON. WDM networks are systems composed of multiple channels, and communication systems which use different wavelengths over the single optical fiber.

The ratio of the data speed to carrier frequency is quite low in optical communication systems (193 THz at the order of gigabit data rate). In this way, many data channel, without having any crosstalk is placed into low-loss window of a single fiber optical cable without having any crosstalk.

WDM-PON is the most “active” method of PON systems. In this model each user (or a group of users) is assigned with a certain wavelength. This means that every subscriber can transmit data to OLT whenever they want independent of the other users. To put it another way, there is no interaction or matching between users in WDM. In this way, problems incurred due to temporal sharing are eliminated.
As a structure, WDM uses wavelength dependent optical splitter for multiplexing and collector is maintained at central office for collecting signals coming to OLTs. Since there is one-to-one connection in WDM there is no need for QoS and MAC algorithms.

WDM has disadvantages as well as advantages. Mux/Demuxes used in ONUs specific wavelength identification should be made beforehand for mux/demuxes used in ONUs. Besides, OLT needs "N" number of transmitters in order to define different connection for "N" number of users.

WDM PON architecture can be divided as follows [14]:

a. Divided Broadband Source
b. Adjustable Laser
c. Reflected Architecture

WDM technology was emerged in the 1970s for the first time and had the commercially most important developments during the 1980s [15].

This technology has become actual main point in terms of increase in bandwidths in networks. ITU communication topology categorizes 72 DWDM channels, at low-loss C band with 100 GHz intervals [16].

A topology of a WDM-PON network is illustrated in Figure 2.5 [13].

Figure 2.5: Schematic representation of the WDM-PON. A single channel acts as entire TDM-PON with sufficient connection points.

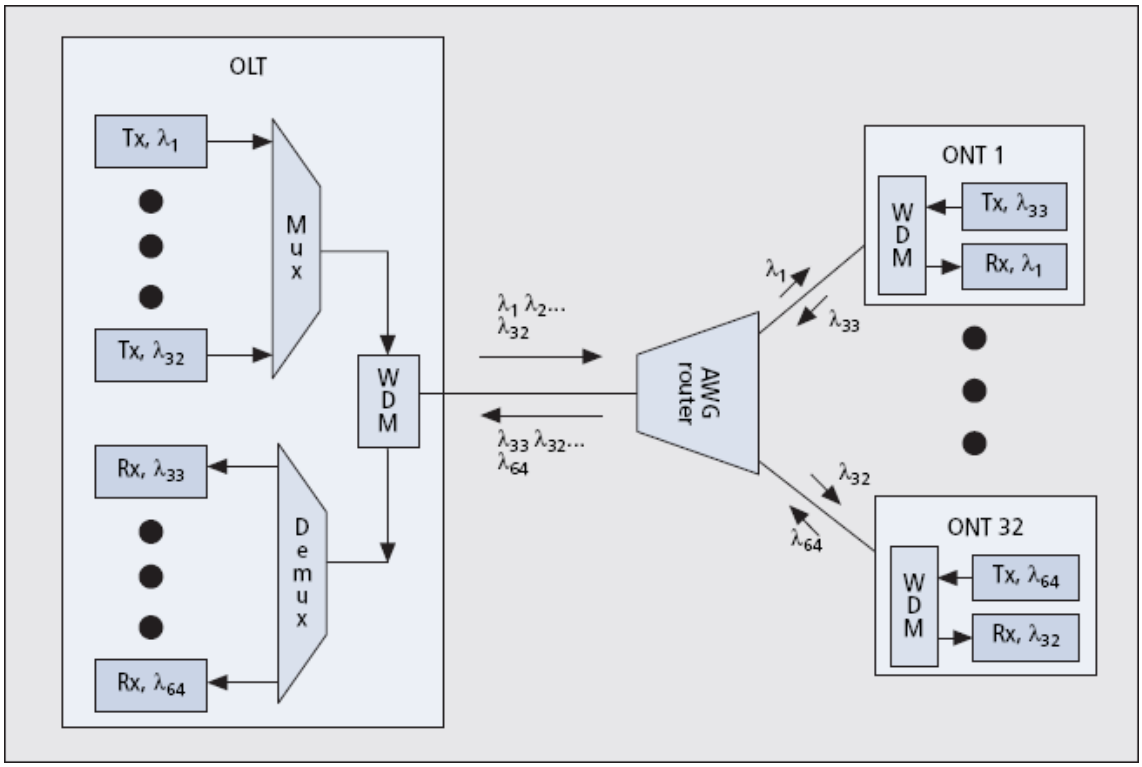

Source: http://front.sjtu.edu.cn/~jinyh/course/Project/PON/Solution.html (14.01.2015)

Thus, each channel may provide a total 1Tb/s bandwidth when it reaches 20Gb/s data flow speed level. This situation is a significant improvement due to use of an effective bandwidth.

By adding AWG's (Arrayed Waveguide Grating) at each end of a single fiber cable, one can connect multiple ONUs to the CO point-by-point. Every wavelength of light travels from CO to ONUs directly satisfying high broadband, ease of modulation and security requirements.

A TDM-PON uses 1310nm wavelength for downstream data typically. For a WDM-PON, there is a need for laser which is able to work at required specific wavelength for every ONU.

In order to have stabilization at wavelength temperature control is important and stabilization is generated at wavelength by having temperature control for every ONU laser.

Elimination of loss mechanism in the system is important in order to increase or expand the coverage of the system, but this requires an amplification process. There is a need for amplifiers due to package-based data traffic and bandwidths which one variable and incremental depending upon and users. Negative consequences of data transmission due to sudden changes in output power and distorting factors at receiver side can be reduced with the use of amplifiers.

Erbium-doped amplifiers which are highly linear amplifiers are classified as amplifiers to serve to this objective for future PON systems. In addition semiconductor optical amplifiers (SOA), amplifiers made up of combination of those and Raman amplifiers are amplifiers proposed for PON systems and metro applications. Although perfect burst-made performance can be attained by using those amplifiers, results have shown that ending-power is limited to 7.5 dBm and it allows communication (transmission) until 60kms. The most recent studies have shown that bi-directional PON links with distributed Raman amplifiers (DRFA) made data transmission possible till 120 km and symmetrical channel data transmission speed reached to 10Gb/s.

With the help of Raman amplifiers, signal weakening is minimized and signal amplification is done at output power. A typical long-distance PON system with Raman amplifiers are shown in figure 2.6 [17].

Figure 2.6: Representation of the long-distance WDM-PON system with Raman amplifiers.

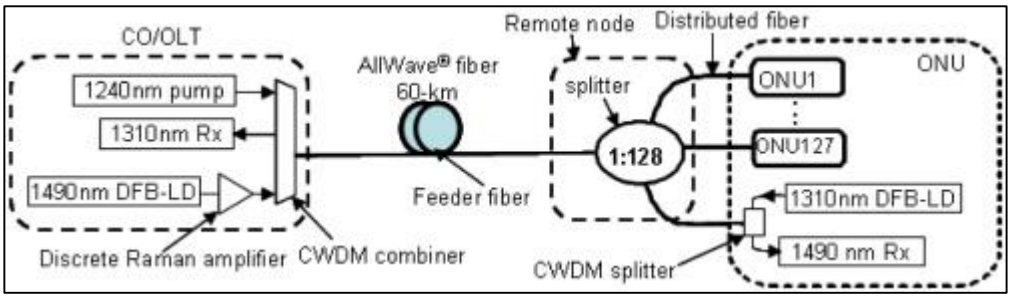

Source: https://www.osapublishing.org/oe/fulltext.cfm?uri=oe-18-22-23428 (29.01.2015)

2.2.3 Central Light Source WDM-PON

This type of WDM-PON was first proposed in 1994, and named as Central Light Source PON [18].

Compared to the WDM-PON system, it provides price advantage as well as several other advantages. CLS-WDM-PON system's principle representation is illustrated in Figure 2.7 [13]. The most important advantage of it is there is no need for specific wavelength source in ONU. In this situation, therefore, there is no need for temperature control within the system in ONU. There only need of frequency adjustment in CO unit.

Figure 2.7: CLS-WDM-PON schematic representation.

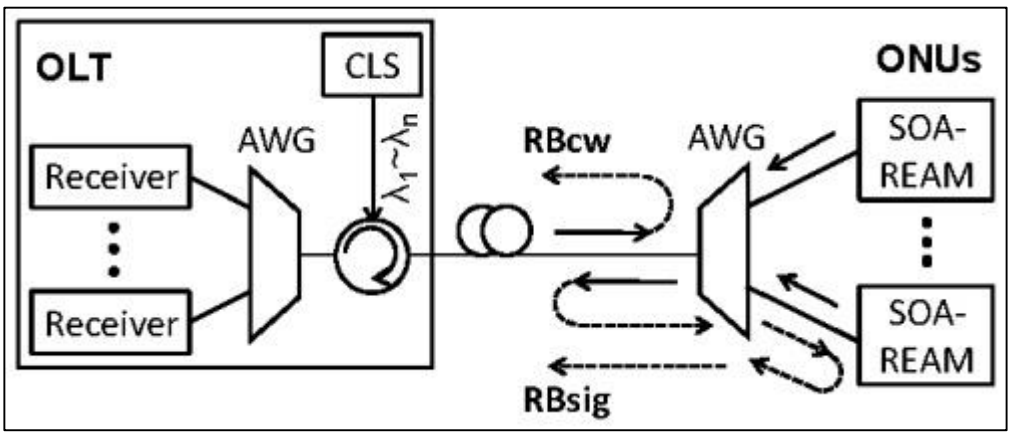

Source: https://www.osapublishing.org/oe/fulltext.cfm?uri=oe-20-26-B452 (03.02.2015)

2.2.4 Code Division Multiple Access (CDMA)

This technology which is also called as fourth generation communication technology allows wireless transportation of high-speed data. It is the optical version of one of the cellular communication technologies. CDMA does not assign a specific frequency to every user. This system allows users to utilize entire frequency spectrum simultaneously by using 0 and 1 bits.

Every user is assigned active and unique transmission code which is encoded by special digital (numerical) system. In this way, service is provided to more users at the same time.

2.2.5 Subcarrier Division Multiple Access (SDMA)

This method performs with P2P connection by attaining different frequencies to every users. In accordance with this, every user sends data to same frequency approximately but at the center these are perceived at different frequencies according to the data. Receiver at the OLT receives N different frequencies and multiplexes as electrical signal. Optical power splitter can be used in here as in TDM models. Use of it makes utilization of n number of users' common wavelength on the single fiber. Utilization of it makes use of common wavelength on the single channel possible for "n" number of users. Even though it seems to be an ideal system at first glance, it has many deficiencies.

2.2.6 PON Applications

These network types are used in industry, and in many application areas. However, creating this network structure and components will be costly as well as be problematic process without having required measurements done. For this purpose, networks structures developed on computer platforms such as Optisystem, Optsim, and Optiwave.

WDM passive optical network transmitters located at the OLT in these programs, making use of photo-detectors filters splitters 1xN OLT's to the structure of the network is distributed more complex example of a simple measurement can be performed at a rate close to reality.

Many different conclusions can be drawn by using BER Analyzer, Optical Spectrum Analyzer or electrical measurement systems. Example, PON circuit is illustrated in Figure 2.8.

Figure 2.8: Example of a PON Circuit

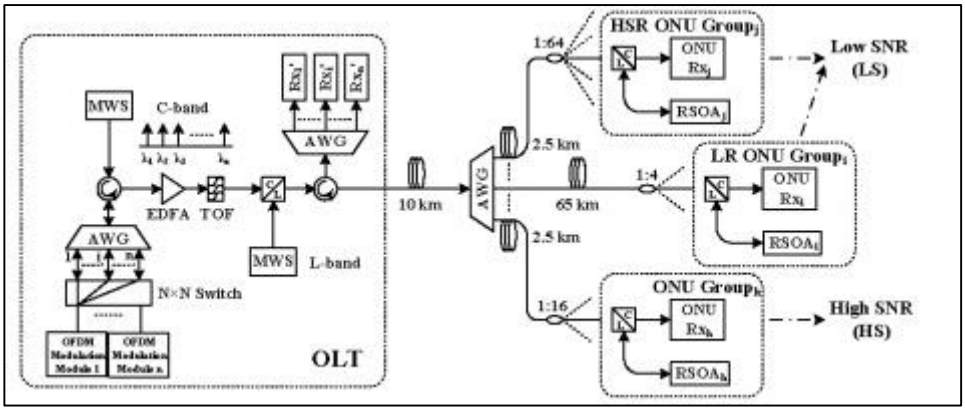

Source: https://www.osapublishing.org/oe/fulltext.cfm?uri=oe-20-23-5284&id=244646 (03.02.2015)

2.3 OPTICAL CONNECTION TYPES

There are variety of units and modules in an optical network. Receiver, transmitter, and optical waveguide which is transmitting the signal one the basic building blocks of optical network. In addition to these, optical modulators, optical sensors, optical filters, optical amplifiers, and optical detectors and soon devices can be used in networks and in many other applications [7].

Network technology can be categorized as point-to-point networks, active element networks with star connection if it is to be examined in terms of its types.

In point-to-point connections, separate lines are installed in order to transmit from central office to every user. Such an approach increases the cost of initial formation of a system but provides maximum flexibility to system's future expansion. It also prepares ground for providing maximum capacity service.

Star-connected active element networks are models in which a single fiber transports traffic to an active node and afterwards of this node independent fiber lines are connected to a cabinet, an apartment or a house [6].
It is cheaper as compared to first model because in order to reach end-user independent fibers are furnished for shorter lengths.

A star-connected passive optical element network is a name given to architecture which is formed by exchanging of active intermediate element in active nodded architecture by a passive optical element.

Figure 2.9: Example of Passive Optical Network Structure

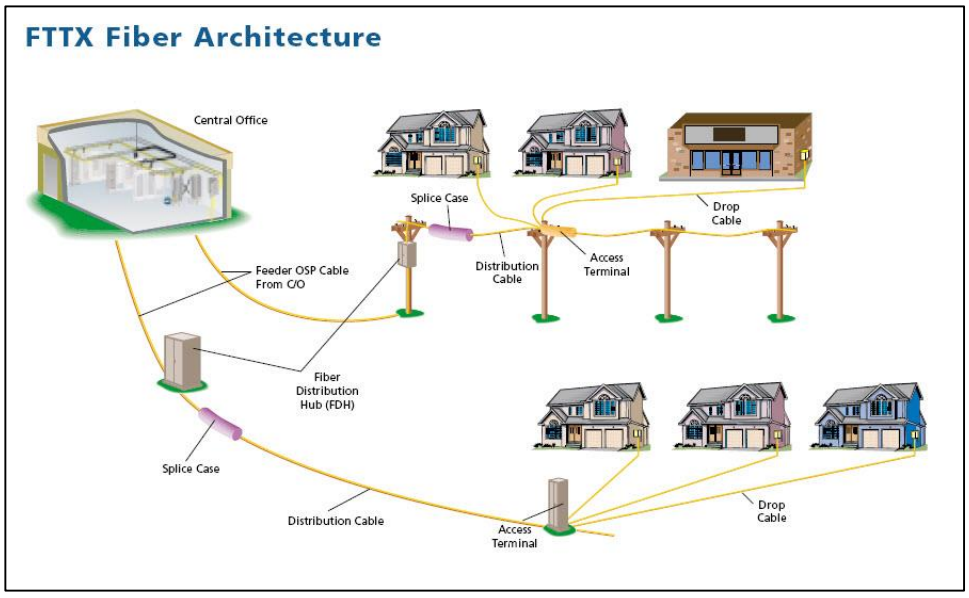

Source: http://www.broadbandsoho.com/FTTx_Tutorial.htm (05.02.2015)

2.3.1 P2P (Point-to-Point Connections)

In this type of connection a different fiber optic line furnished to every user separately over central office [6].

With the help of this line receives will have high capacity internet. The advantages of a system is being open to any kind of improvements and having high capacity. The disadvantage of a system is that furnishing different fiber lines to every user makes it costly.

2.3.2 P2MP Active Star Connections

In this type of connection fiber line from central office goes to certain node point and service recipients are served from this node.

The advantage of the system is that it is less costly due to the use of fiber line from center requires lesser use of cable. The disadvantage is higher maintenance cost of intermediate node points.

2.3.3 P2MP Passive Star Connections

The difference of this type of connection from active star connections is replacement of active element at node point with passive distributor element. The advantage of the system is that cost of maintenance of the active element.

With Raman amplifiers bit speed of 10Gb/s (gigabit per second), 1024 split factor values and 135 km link lights can be reached and even exceeded in PON systems.

Figure 2.10 illustrates a PON with long distance access Distributed Raman Fiber Amplifier (DRFA) [19].

In hence, single fiber, bi-directional and back-haul link system is shown. Optic line terminator (OLT) is connected to metro network core node. The length of system with back-haul link is approximately between 50-100 km.

Figure 2.10: Representation of Passive Optical Network Structure

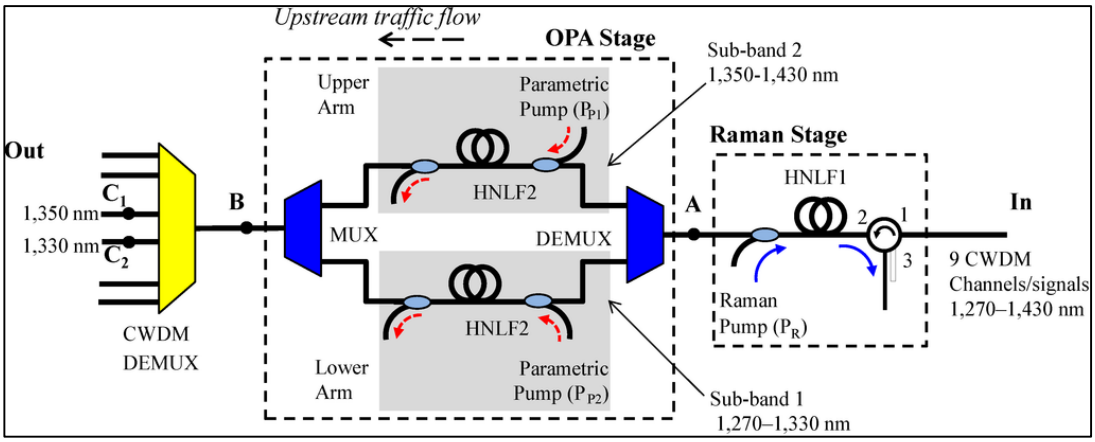

Source: http://www.mdpi.com/2304-6732/1/4/473/htm (07.02.2015)

2.4 SCATTERING MECHANISM IN FIBER OPTIC

2.4.1 Introduction

In data communication with optical fiber cables some of the photons are scattered backwards when light is propagating through fiber. This scattering which occurs in fiber structure emerges as Rayleigh scattering which results from interaction of material structure heterogeneity and changes in fiber density in silica structure with photons or as Raman or as Brillouin scattering which are resulted from an interaction of photons with molecular and volumetric vibrations.

Backward-scattering of photons are combination of these three scattering mechanisms. In other words, the total effect of Rayleigh, Brillouin and Raman scattering can be seen on backwards-scattered optical signal.

Rayleigh scattering, which is less sensitive to changes in temperatures issued in determination of losses, refractive and heterogeneity mostly, Raman and Brillouin scatterings are used widely in detection of formation of tension and temperature.

Light scattering is classified as elastic scattering if the frequency of the input photon and the frequency of the scattered photon are the same, and as inelastic scattering if those frequencies are different. Rayleigh scattering is an example for elastic scattering, Raman and Brillouin scatterings are examples of inelastic scatterings.

When the fiber optic cable is used as a detector, Brillouin scattering is less sensitive to the temperature change as compared to Raman scattering but it is more sensitive to changes in the tension.

1550nm wavelength scattering mechanisms in optic fibers are shown in Figure 2.11.

Figure 2.11: Schematic representation of frequency spectrum for Raman, Rayleigh and Brillouin scatterings in optical fibers.

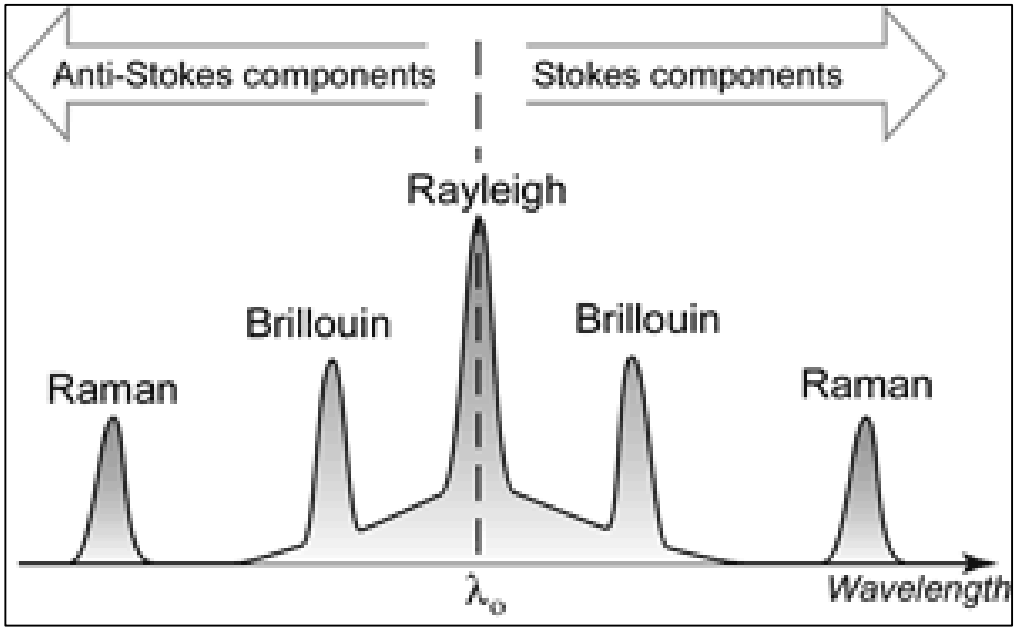

Source: http://www.omnisens.com/ditest/362-bst.php (10.02.2015)

Components of Brillouin are 15dB smaller than Rayleigh components approximately in 1550nm and there is 11GHz frequency difference between them. There is approximately 13 THz frequency difference between Rayleigh and Raman components.

Data losses and signal weakening are occurring in optical fibers in data transmission. The power of light signal becomes weakens at the exit due to the non-linear effects such as backwards Rayleigh scattering and backwards Brillouin scattering while moving through fiber.

Because of this, there can be weakening in bi-directional transmission due to non-linear effects from backwards scattering in passive optical networks (PON).

2.4.2 Brillouin Scattering

Brillouin scattering is the scattering mechanism which is explained as backwards scattering resulting from interaction of photons traveling through fiber optical cable and the spontaneous acoustic waves occurring due to the changes in the fiber structures. Mirrored light shifts to the different frequency as in the case of Doppler since acoustic wave is moving through the fiber. Therefore, there will be a frequency shift between moving photons and back-scattered photons.

In other words, spontaneous Brillouin scattering is light scattering from acoustic waves which are spreading in the environment. Applied optical field is too weak to change the material properties of the environment. Light is interacting with acoustic waves while moving. Acoustic waves occur in a wide frequency range; however frequencies satisfying the Bragg condition which are resulting in efficient pump light scattering, are more important. Light scattered in this situation is exposed to downstream Doppler frequency shift. To put in another way, the anti-stokes light propagation is composed of similar mechanism coming from acoustic wave approach [20].

Frequency shifts which express Stokes and anti-Stokes operations are given below respectively.

$$\nu_{s,\,as} - \nu_p = \mp \nu_a \qquad (2.1)$$

In here, v_s is the Stokes frequency, v_{as} is the anti-Stokes frequency, v_p pump frequency and v_a is the acoustic frequency. In addition "±" symbols are applied to Stokes and anti-Stokes components respectively. In other words, the Brillouin frequency shift magnitude is equivalent to the acoustic frequency.
Scattering occurs in all directions, but signal scattered backwards axially is guided at fiber entrance backwards only.

2.4.2.1 Spontaneous Brillouin scattering

Brillouin scattering occurs as a result of interaction of thermal effects in the system occurred in the environment acoustic waves occur in silica glass fiber structure and pump photons pumped into optical fiber. In this case, photon lights advancing in the fiber are scattered backwards by clashing acoustic waves.

Brillouin backward-scattered stokes' and anti-stokes', especially for anti-stokes, total power can be found by photo detectors for backward-scattered (180 degree opposite direction) at backward direction at the end of the fiber. Thus, signal power and their data loss can be found by comparing exit signal power detected by photo detectors and entrance signal injected by the laser into the fiber [21].

Brillouin scattering takes place spontaneously. Light wave injected into fiber interacts with acoustic waves which is taken place thermally in the environment and results in light scattering (phonons and photons), and this is called as Brillouin scattering.

In the other words, it can be considered as diffraction of light resulting from refraction index differences due to acoustic waves in fiber. Acoustic waves formed thermally emerge on frequencies defined over a wide range with separate phonon energies [21].

In figure 2.12 Brillouin scattering is shown which takes place interaction between light wave advancing in fiber with acoustic wave resulting from thermal effects [21].

In the figure, λ_p is pump wave length, λ_{bs} Stokes wavelength, λ_a acoustic wave length and θ is the angle between pump and stokes wave vectors. In here, spontaneous Brillouin scattering with frequency shift depending on scattering angle occurs where incoming optical wave is phase compatible with acoustic wave and the condition given in equation 2.2 is valid [21].

Figure 2.12: Brillouin scattering resulting from interaction between acoustic wave with light advancing in fiber.

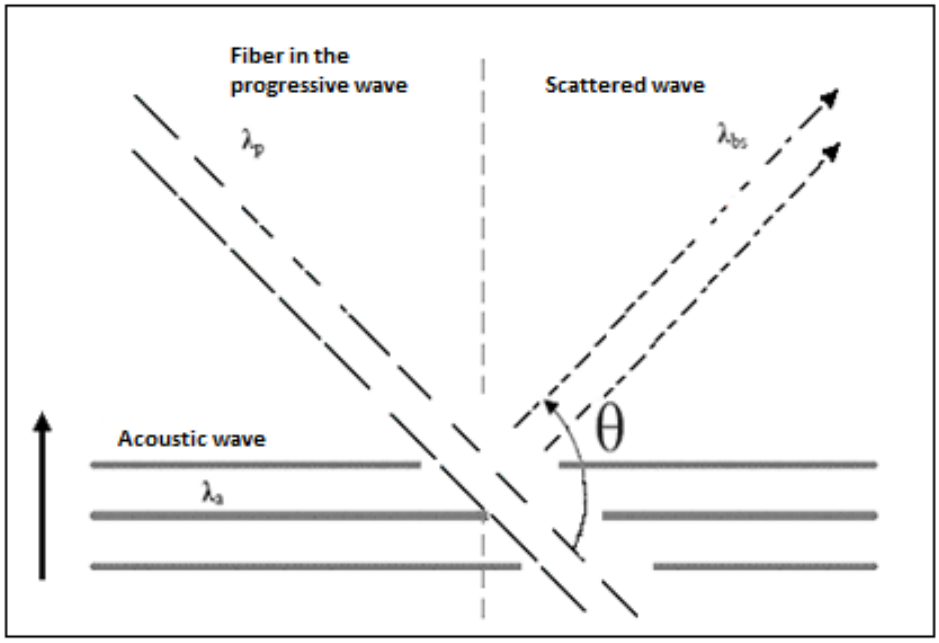

Source: M. Alahbabi, distributed optical fiber sensors based on the coherent detection of spontaneous Brillouin scattering, PhD Thesis, 2005.

This situation can be seen by analyzing Bragg diffraction wave vectors belong to three types of waves shown on Figure 2.12.

$$2n\lambda_a \sin\frac{\theta}{2} = \lambda_p \qquad (2.2)$$

Acoustic wave λ_a, as in the previous section, is formulated as follows:

$$\lambda_a = \frac{\upsilon_a}{f_a} \tag{2.3}$$

In the equation υ_a is acoustic wave speed. Acoustic frequency f_a can be expressed as follows from these equations and this expression satisfies the Bragg condition.

$$f_a = \frac{2n}{\lambda_p}\upsilon_a \sin\frac{\theta}{2} \tag{2.4}$$

Equation (2.4) stands for a numerical value for frequency shift resulting from scattered light from acoustic waves.

As it is shown in equation 2.4, in the case where $\theta = 0°$, there will be no frequency shift. However, in opposite direction, in other words, when $\theta = 180°$ Brillouin frequency shift will be maximum.

For example, Brillouin frequency shift reaches to the maximum at this wavelength by using known $n = 1.46$, $v_{a\,=\,5960m/s}$ and $\lambda_p = 1550nm$ values and this is the value where Brillouin frequency shift is f_a =11.2 GHz.

Frequency shift is dependent on speed of acoustic wave as well as on light moving in fiber, on angle between light and mirrored light and on fiber refraction index.

Scattering is guided both forward direction and backward direction fiber optic. As a result, acoustic frequency *fa*, has the maximum value when light is scattered opposite to the direction of advancing light wave in fiber. θ angle will be 180 in here [20].

Brillouin frequency shift *vb*, is equivalent to acoustic frequency *fa* and therefore *fa* statement takes the following form:

$$\upsilon_b = \frac{2n}{\lambda_p}\upsilon_a \tag{2.5}$$

$$g_B(v) = g_b \frac{(0.5\Delta v_b)^2}{(v - v_b)^2 + (0.5\Delta v_b)^2} \tag{2.6}$$

Here, Δvb Brillouin gain line width at 1550 nm on silica fiber is approximately ≈ 35 MHz, vb given by Equation (2.6) is Brillouin frequency shift and gb is Brillouin gain coefficient for $v = vb$ and it is expressed as follows:

$$g_b = \frac{2\pi.n^7 p^2}{c\lambda^2 \rho v_a \Delta v_b} \tag{2.7}$$

In equation (2.7), v_a is acoustic wave velocity, c is the speed of light in the space, n is fiber core refraction index, ρ is the material density of the fiber.

In equation, gain coefficient can be calculated by putting values silica fiber parameters at 1550nm as $g_b \approx 5x10^{-11}$ m/W.

Three parameters that characterize the spectrum of the Brillouin gain are Brillouin gain coefficient, Brillouin line width, and Brillouin frequency shift. There is also Brillouin frequency spectrum peak at single mode fiber (SMF) and it is in the form of a Lorentz function.

Brillouin gain coefficient and parameters such as power end line width change depending on material structure of fibers and physical effects.

2.4.3 Rayleigh Scattering

Rayleigh scattering is a scattering mechanism occurring throughout the entire fiber. It is resulting from irregularities, random heterogeneity at density and frozen composition variations in optical fiber at the production stage [21].

These changes in fiber result in fluctuation of refraction index and the numerical range of the optical fiber (NA, is a parameter depending on the core and the cladding refractive indices.) the scattered light, a portion of the fiber light wave advancing in the opposite direction, resulting in guiding.

Rayleigh scattering is characterized by attenuation coefficient of α. This coefficient is proportional to λ^{-4} for standard single mode fiber at 1550nm. Here $\alpha \approx 4.56x10^{-5} m^{-1}$ and is α is equivalent to ≈ 0.20 dB/km of fiber attenuation [21].

2.4.4 Raman Scattering

Inelastic scattering processes such as Raman emerge as a result of interaction between light sent inside fiber and vibrational molecular modes arising from environment's molecular structure. The energy change of the photons can be explained by phonon interactions [21].

In this process, both energy loss and energy gain can occur. If there is a reduction in the energy (or in the frequency) Raman stokes components are generated, if there is an increase (or in frequency) then Raman anti-stokes components are generated.

Figure 2.13(a) indicates schematic diagram of Rayleigh scattering in a silica fiber, and Figure 2.13(b) shows Raman scattering in silica fiber.

Figure 2.13: Molecular vibration energy levels. (a) Rayleigh Scattering (b) Raman Scattering in silica fiber. In Figure, v_o and v_1 stand for incoming light frequency and scattered light frequency respectively, h stands for Planck constant.

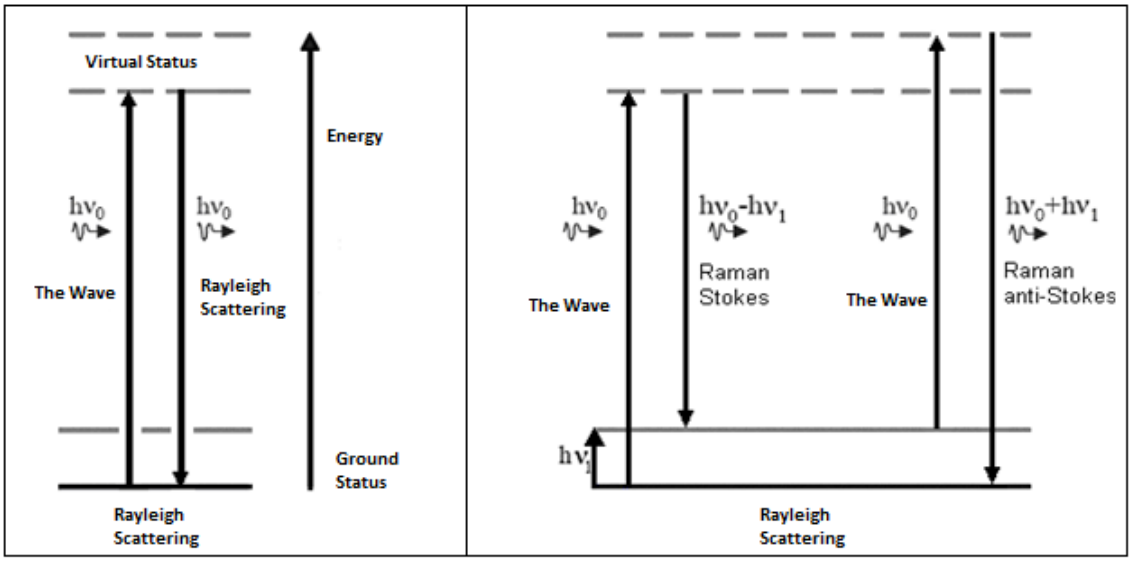

(a) Rayleigh Scattering (b) Raman Stokes and anti-Stokes Scattering

Source: M. Alahbabi, Distributed optical fiber sensors beased on the coherent detection of spontaneous Brillouin scattering, PhD Thesis, 2005.

Raman scattering in optical fiber data communication emerges in wide frequency range due to non-crystallization of natural structures of molecules in glass cage and different vibrational energies are guided for different molecule groups in glass structure.

This important feature of Raman scattering allows Stokes and anti-Stokes spectra to be broad-band [21].

Raman scattering has a significant share in signal weakening amongst other scattering mechanisms.

Energy level density of phonons in scattering is influenced by phonon dispersion (in a situation of increase/decrease in temperature).

The change in the backward scattered Raman signal power with the temperature is shown as a function of temperature in equation 2.8 [22].

$$R(T) = \left[\frac{\lambda_s}{\lambda_{as}} \right]^4 e^{-(\frac{h\Delta Vr}{kT})} \qquad (2.8)$$

Here, λ_s and λ_{as} are Raman Stokes and anti-Stokes wavelengths respectively, h is Planck constant, Δv_r is frequency difference between Raman anti-Stokes and pump, k is Boltzmann constant, and T is the temperature in Kelvin.

In the frequency domain, Raman scattered signal photons are composed of stokes scattered signal photons and anti-Stokes scattered signal photons. Raman Stokes and anti-Stokes signal frequencies can be expressed as it is given in 2.9.

Stokes Scattered Frequency

$$fs = fo - \Delta f \qquad (2.9)$$

Anti-Stokes Scattered Frequency

$$f_{AS} = fo + \Delta f \qquad (2.10)$$

In this expression, fo frequency of incident light Δf is frequency shift and $\Delta f = 13.2x10^{12}$ Hz for silica.

During the Raman scattering, photon goes from initial steady state to another steady state and energy difference is $\Delta E = h.\Delta f$. Here, h is Planck constant and Δf stands for frequency differences between levels.

In single-mode fibers, effective power attenuation coefficients for Stokes and anti-Stokes waves are given by equations 2.11 and 2.12.

$$\alpha_{P,S} = \frac{\alpha_P(\lambda_0) + \alpha_P(\lambda_S)}{2} \tag{2.11}$$

$$\alpha_{P,AS} = \frac{\alpha_P(\lambda_0) + \alpha_P(\lambda_{AS})}{2} \tag{2.12}$$

Attenuation coefficient for parabolic gradient index multimode and single-mode fibers for different wavelengths are given on Table 2.1.

Figure 2.14: Ranges of attenuation coefficients of silica glass single-mode and multimode fibers.

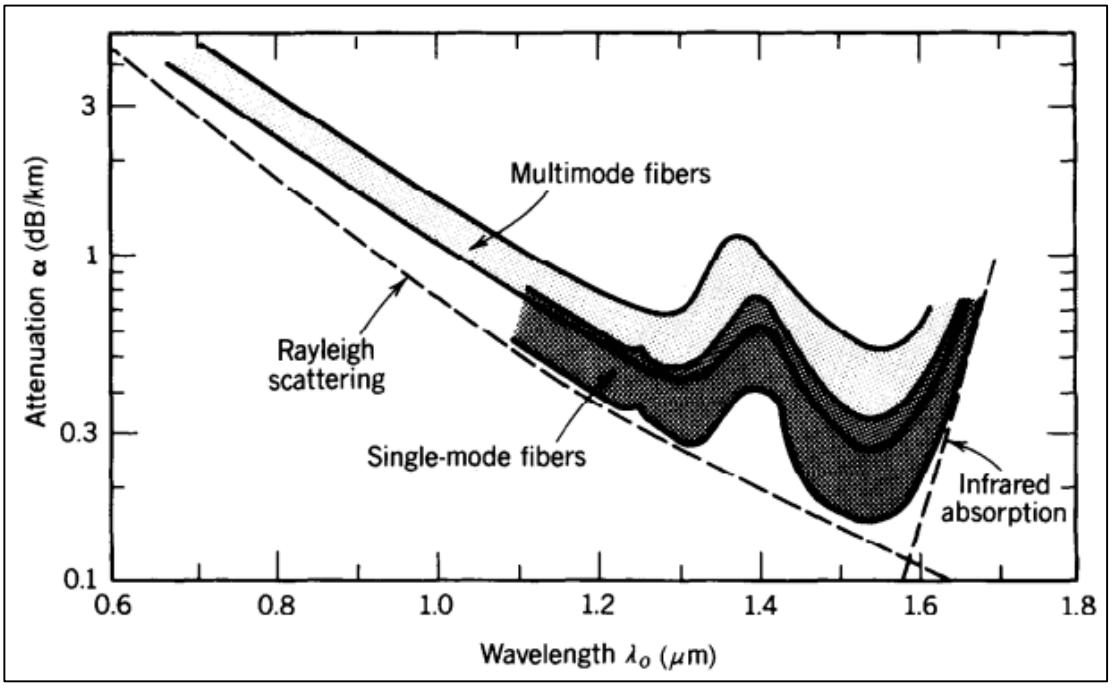

Source: http://opt.zju.edu.cn/zjuopt2/upload/resources/chapter8%20Fiber%20Optics.pdf (10.02.2015)

Stokes and anti-Stokes attenuation coefficient is expressed by Neper with $\alpha_{P,S}(neper) = \alpha_{P,S}(dB)x\frac{\ln(10)}{L}$ equal. Fiber length is expressed by L.

2.5 BACKWARDS-SCATTERING PRICIPLE-BASED OPTICAL MEASUREMENT TECHNIQUES

Optical time domain reflectometer (OTDR) is well-known technique which is used to characterize fiber losses incurring along the optical fiber.

A light pulse is sent into the optical fiber, and then Rayleigh backwards-scattered signal through optical signal entry point is captured and measured [20].

This temporary information can be converted into spatial information which has the back-scattered fiber data, as in the case of loss mechanisms occurring outside the fiber throughout the fiber (splice losses, bending losses, connector losses, and bends), in election to inward fiber losses.

ODTR technique is advantageous because measurements can be done from one end of the fiber.

2.5.1 OTDR Principle

OTDR principle can be understood as evaluation of short pulse duration (w) expending in fiber optic. Light is exposed to linear scattering losses mainly resulting from Rayleigh scattering as it moves in fiber. This scattering is emerges as a result of material composition fluctuations existing in glass cage frozen at fixed temperature and material heterogeneity [21].

These fluctuations occur at a small scale compared to the wavelength of the light. Scattering occurs in all directions but only small part of it can be captured from fiber's numerical aperture and it is guided backwards to fiber's entry point.

Rayleigh scattered signal density is elastic scattering as well as it is inversely proportional fourth power of wavelength (λ). Therefore, it occurs at the same frequency and polarization light sent into the fiber. In modern silica-based optical fibers Rayleigh

scattering is dominant loss mechanism and at 1550nm (approximately) 0.18 dB/km values contributes to signal weakening.

It is possible to determine the scattering point by measuring reflection (mirroring) duration of light in OTDR method. If light scattering time is "t" in backward and forward directions, the path of light can be found by $d = ct/2n$ formula.

Rayleigh backward scattered signal power $P_R(t)$ is given as a function of time in the following formula:

$$P_R(t) = \frac{S}{2} P_i \gamma_R w v_g e^{-\gamma v_g t} \tag{2.13}$$

In this equation, backward scattered signal power as a function of distance $P_R(z)$, (z) can be obtained by using $t = 2z/v_g$ equation.

$$P_R(z) = \frac{S}{2} P_i \gamma_R w v_g e^{-2\gamma z} \; ; \tag{2.14}$$

$$S = \frac{(NA)^2}{4n^2} \tag{2.15}$$

where,

S : Back scattering capturing coefficient

P_i : Input signal power

γ_R : Rayleigh scattering coefficient

γ : Fiber attenuation coefficient

w : Temporal pulse width

v_g : Group velocity of light moving inside fiber

t : Time

NA : Fiber numerical aperture

n : Core refraction index

In the expression of P_R for Rayleigh power is shown logarithmic change of optical power on Rayleigh power. Reflections generate an increase and then a decrease in signal level, and fiber losses result in reduction in signal level.

2.5.2 BOTDR Principle

Brillouin optical time domain reflection meter (BOTDR), similar to the OTDR principle, based on the principle where thermal effects resulting from the acoustic waves in the fiber based on the principle of light scattering by interacting sent.

In contrast to Rayleigh scattering, it is not a scattering resulting from density fluctuations. Similar to backwards scattered Rayleigh signal, Brillouin signal shows same logarithmic attenuation as time elapses depending on wavelength of the light.
BOTDR principle enables detection at longer distances, but it has constraints in temperature and spatial resolutions. A general BOTDR system is shown in Figure 2.14 [23].

Figure 2.15: Typical configuration for a BOTDR system. FUT is the fiber under test or distributed transducer, LO is the local oscillator, and CW is the continuous wave.

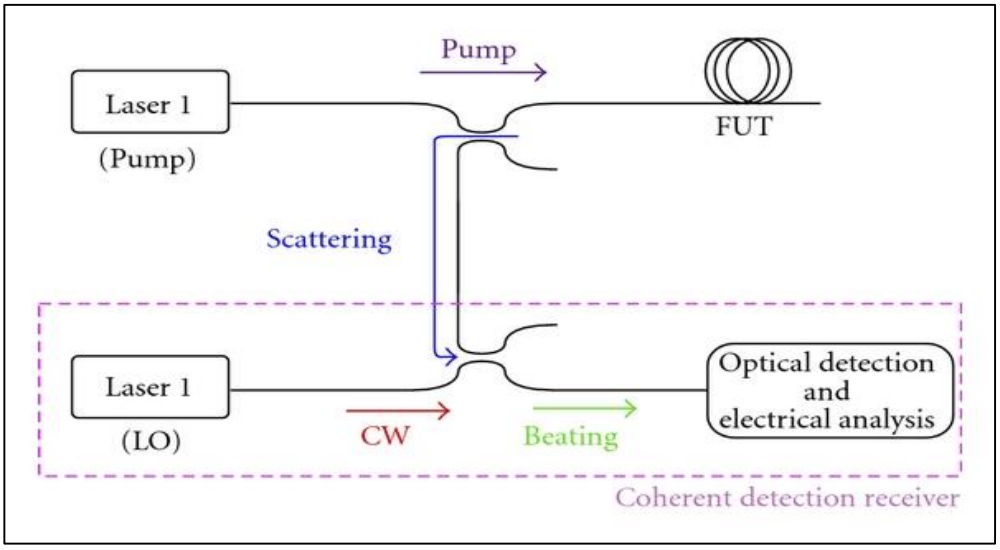

Source: C. A. Galindez-Jamioy and J. M. López-Higuera, Brillouin distributed fiber sensors: An overview and applications, Article ID 204121, 2012.

In order to increase the capacity of fiber sensors, decreasing the loss of Brillouin sign between the receivers decreasing the loss of techniques are available for this purpose. Mach-Zehnder interferometric filtering method is a method widely used for this method and it is one of the reliable methods.

These interferometers can be single-pass and double-pass configuration. This method enables distinguishing backwards scattered Rayleigh and spontaneous Brillouin signals at low losses and at high resolution.

3. MATERIAL AND METHOD

3.1 INTRODUCTION

In data communication with optical fiber, besides non-linear optical influences such as Rayleigh, Raman and Brillouin scattering signal reduction may also result from fiber loss mechanisms such as non-linear phase modulation, four waves mixing and signal absorptions by silica material of fiber.

To talk about adverse effects of abovementioned influences may be possible because fiber cables are also used for data communication process via passive optical networks.

During data communication two important factors of the communication channel usually influence communication. These are distortion and noise.

If signal change in a channel can be expressed by only multiplying with a coefficient and/or a time delay this channel may be deemed without distortion, otherwise that communication channel has a distortion [24].

Another important influence on a communication channel is random noise. Signal transmission or transfer occurs very easily in a noiseless environment. However in practice random noise always appears. In applications and/or designs some precautions which enable to recognize the signal from the noise are taken. For this purpose some constructions and system infrastructures with complex structure are used.

If the main purpose of a communication system is transmission of information from one point to another; to explain relative superiority and performance of the systems without measuring quantity of transmitted information via communication lines (including among units in PON links) will not be possible. This question can be answered by studying and explaining the relation between information and bandwidth that is also included in the information theory.

During data transmission on PON, transmission disorders (distortion), overlapping and affecting the signal, and noise which means unwanted signals, transmission reduction or loss also result in decrease in performance of transmission line and affects transmission characteristics of the PON systems.

In communication, for transmission of information to be unchanged and originally without distortion, following conditions must be ensured for receiver output signal:

a. Output signal is a form of input signal of which amplitude is increased or decreased. Namely, there is not any deformation.

b. Output signal is a form of input signal which is shifted a little on the timescale axis. Namely, there is a delay. Because of finite propagation speed of electromagnetic events, a zero delay is not possible.

Distortions on communication systems are classified as linear distortion (reducing and phase distortion), harmonic distortion and modulation distortion. Harmonic distortion is the distortion resulting from nonlinearity of transmission environment via which information is transmitted. In such cases, in addition to distortion in amplitude and phase of the signal a change in the frequency of the signal also appears. Such systems are referred to as nonlinear systems.

If a signal of information signal with frequency f1 is applied to input of such a transmission system or a PON system, in the output side of the system harmonic frequencies such as f2, f3, f4 will appear besides the main frequency f1. If u_1 represents the amplitude of the main frequency and u_2, u_3, u_4, ….. represent amplitude of the harmonic frequencies, then the harmonic distortion coefficient is defined as follows:

$$k = \frac{\sqrt{u_2^2+u_3^2+u_4^2+\cdots}}{u_1} \quad \text{or} \quad k = \frac{\sqrt{u_2^2+u_3^2+u_4^2+\cdots}}{\sqrt{u_1^2+u_2^2+u_3^2+\cdots}_1} \tag{3.1}$$

Modulation distortions emerge because phase and amplitude responses of transmission environment change in the course of time. This goes into two divisions, Amplitude distortion and Phase modulation distortion.

Reduction throughout the transmission way varies depending on the length of the way and frequency components in the signal [24]. For instance, during transmission of a speech an extreme reduction of high frequency components in the signal affect conversation. Therefore reduction should be equal for all frequency components. In order to ensure this, in other words to correct the disorder an electronic circuit which correct the associated with the frequency is placed at the end of the way. This device, called balancer, results in a change contrary to the line. Thus, all frequency components have the same reduction characteristics. Consequently, different reduction influence of the signal on various frequency components is prevented and the spectral shape of the signal is conserved.

In the most general sense, noise in communication networks and/or data transmission involves unwanted signals in communication systems. This is the most important factor restricting system performance. Noise is classified as thermal noise, intermodulation noise, diaphony (cross talk) noise and impulse noise.

Thermal noise exists in all transmission environments and in all communication devices. It occurs because of random movement of free electrons in a conductor such as a resistor due to the temperature.

If the temperature is above absolute zero (-273 °C) noise always exists. It is a parameter of determination of lower limit of sensitivity of receiver system.

3.2 NOISE AND FIBER LOSES

Noise is an unwanted disorder which masks our received signal; therefore it reduces performance of the detection system. Noise source on PON links is a combination of electrical and optical noises. Thermal noise (noise resulting from temperature), impulse

noise and quantum noise are the forms of electrical noise and it appears on detector and receiver-transmitter systems. In general, quantity of electrical noise can be reduced by averaging the signal. Optical noise sources are Coherent Rayleigh Noise (CRN), Polarization Noise, Relative Intensity Noise (RIN) and Amplified Spontaneous Emission (ASE) Noise. Other optical noises apart from RIN cannot be reduced by averaging the signal. Amplified Spontaneous Emission (ASE noise) will appear if optical amplifiers are used on the detector system.

Coherent Rayleigh noise appears as fluctuations on the lines of Rayleigh reverse scattered signal intensity. It is the main source of the noise and occurs when a source with narrow bandwidth is used.

Widely used signal averaging techniques are not used effectively for the purpose of reducing CRN. However the noise can be minimized significantly by using a broad band impulse source and averaging numerous signals. This technique is named as Frequency Shift Averaging (FSAV).

Polarization noise, in other words losses in the components of the system associated with polarization, appears as fluctuations in Brillouin intensity lines. This noise is detected by Coherent Detection method because standard single mode fiber has low birefringence. Consequently, in case of polarization of Brillouin signal and the local oscillator which results in such noise differential changes appear.

Noise can be reduced significantly by choosing light polarization randomly (either in both of probe and reference sources or in any one of them). Furthermore, reducing the noise is possible by using FSAV technique. RIN appears as random fluctuations in output intensity of semiconductor injection lasers. Such fluctuations turn into optical intensity noise.

ASE noise appears in detector systems where EDFA (erbium doped fiber amplifier) or Raman amplifiers are used.

As is known, bandwidth of EDFA and Raman ASE are ≈ 50 nm and ≈ 100 nm respectively. Broad signals affect Brillouin signal by creating noise signals in impulse frequency during mixing process. These mixing processes are named as ASE-ASE impulses, ASE-local oscillator and probe-Rayleigh signals (ASE-Signal). In general, as in ASE-ASE noise components can be reduced by using narrow band Bragg grating optical filters. ASE-probe impulse noise cannot be reduced by using narrow band filtering method.

Total measurement time varies depending on the time spent for summing up or processing single lines and the time spent for multiplying with average in order to reach at the required SNR rate. As is known, there is a relation between data averaging time and detector performance which varies depending on detector application type. However, high repetition rate and rapid data acquisition systems shorten measurement time significantly. Because of necessity of optical amplification in both transmission and receiving end of fiber detector, in order to ensure use of low loss window selected wavelength should be optimized in such a way that it corresponds to the third window (1550 nm window). However, approximately 0.40 dB/km fiber losses are unavoidable when this wavelength is even 1550 nm. For instance, for a 100 km long fiber detector Brillouin signal can be reduced to 40 dB. Therefore fiber loss is an important factor influencing detection distance.

3.3 NON-LINEAR EFFECTS

In a BOTDR based distributed fiber detection reverse scattered signal is proportional to impulse energy in the fiber. Impulse energy varies depending on impulse width and peak intensity value. However, required spatial resolution restricts impulse width. In spite of existence of the sources with high peak intensity maximum peak intensity applied in the fiber is limited with the requirement of avoidance of non-linear effects.

When intensity threshold is exceeded non-linear effects affect the form of reverse scattered signal lines either directly or by changes in pump reduction and/or probe spectral expansion. Such distortions result in errors in measurements. Important non-

linear effects to be considered are; Stimulated Raman Scattering (SRS), Stimulated Brillouin Scattering (SBS), Self Phase Modulation (SPM), Four Wave Mixing (FWM) and Modulation Instability.

3.4 COHERENT RAYLEIGH NOISE

CRN reduces signal/noise ratio of a FODTS which is not limited to receiver noise. Therefore CRN provides a significant limitation on detector accuracy and reachable temperature resolution. In this document ways of elimination of CRN are studied. To determine the quantity of CRN frequency shift averaging process and an analysis method developed by Horiguchi in order to reduce the noise on reverse scattered Rayleigh signal in a fiber [24].

In a FODTS RMS CRN (f_{CRN}) can be expressed as a part of Rayleigh signal as follows:

$$f_{CRN} = \sqrt{\frac{v_g}{4\Delta z \Delta v}} \tag{3.2}$$

In the equation, v_g is the group speed of the light in the fiber, Δz is spatial resolution and Δv is frequency shifted bandwidth of the source. Spatial resolution can be expressed as indicated in equation (3.3).

$$\Delta z = \frac{w v_g}{2} \tag{3.3}$$

In the equation, w is temporal pulse width.

Equation (3.3) which indicates percentage of CRN on reverse scattered Rayleigh beam is the expression of group speed, spatial resolution and bandwidth of the source.

3.5 ANALYSIS OF COHERENT RAYLEIGH NOISE

Coherent Rayleigh Noise (CRN) limits signal/noise ratio of a FODTS which is not exposed to a limitation of any electronic noise. However, when CRN is considered as a function of the bandwidth a reduction in CRN depending on increase in bandwidth is observed. Furthermore these results show that theoretic approaches are consistent with experiment results.

In addition to this, FODTS with different laser bandwidth and different spatial resolution are studied. According to study results, an increase in source bandwidth and/or spatial resolution results in a decrease in CRN and these are consistent with the theoretic prediction.

In Figure (3.1) three vertical Rayleigh lines are shown for a net illustration. From the top to bottom, 3 MHz, 1 MHz and 270 kHz bandwidths are shown respectively. In the illustration, it is clearly seen that CRN is reduced by decreasing the demodulation bandwidth.

In fibers longer than 500 meters reduction of Rayleigh signal is negligible and is approximately ≈ 0.2 dB and percentage of noise quantity can be calculated by RMS voltage ratio on horizontal lines on a proper environment signal.

Second column of Table 3.1 indicates percentage CRN calculated theoretically.

Figure 3.1: Narrow band Rayleigh signal calculated in different spatial resolutions.

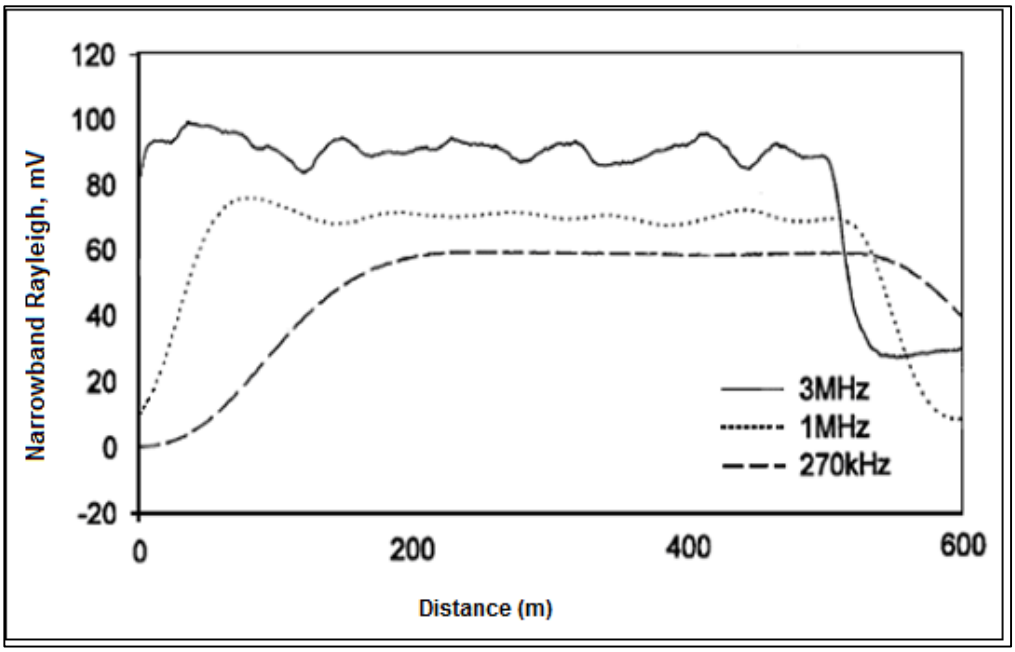

Source: K. De Souza, Significance of coherent Rayleigh noise in fibre-optic distributed temperature sensing based on spontaneous Brillouin scattering, 2006.

f_{CRN} Coherent Rayleigh noise is calculated as follows by using spatial resolution values $v_g = 2x10^8$ and $\Delta v = 2GHz$ for 1.5 meters (15ns), 3m and 5m:

$$f_{CRN} = \sqrt{\frac{v_g}{4\Delta z \Delta v}} = \sqrt{\frac{2x10^8}{4x1.5x2.10^9}} = 0.129 \qquad (3.4)$$

In this calculation Coherent Rayleigh noise is found 12.9 percent similarly; Rayleigh noise values for 3m and 5m spatial resolution respectively are indicated in Table 3.5.

As seen from the equation, Coherent Rayleigh noise can be reduced by increasing spatial resolution.

Table 3.1. Theoretical CRN percentage in different bandwidths.

Bandwidth	Theoretical CRN Percentage
3MHz	12.9
1MHz	9.1
270kHz	7.0

Source: K. De Souza, Significance of coherent Rayleigh noise in fibre-optic distributed temperature sensing based on spontaneous Brillouin scattering, 2006.

In a fiber optic distributed temperature detector based on Landau-Placzek ratio case is different. In such detection system, by using a narrow band Q-switched erbium doped fiber laser with stimulated broad band capacity and integrating with a SPZM with loss less than <1dB reaching at higher performance is possible. By using SPMZ very low losses in reverse scattered signals will be possible and thus signal/noise ratio can be increased as such in Rayleigh signal.

3.6 NOISE SOURCES IN SIGNAL DETECTION SYSTEM

In a direct detection system with erbium doped fiber amplifier, identifiable major noise sources are indicated below.

i. Photodiode Noise

Photodiode noise consists of the followings:

a. Photo current and dark current impulse noise,
b. Thermal noise of diode resistance.

In semiconductor photo diodes free electrons and holes occur randomly and conjugate. This results in impulse noise current. Impulse noise consists of two components; one of them is created by optical input signal to photo diode and the other one result from the dark current which naturally occurs due to thermally creation of electron-hole couples.

This noise is a white noise on detection bandwidth. In addition to this, measurable and small photo diode resistance creates a relatively small and negligible thermal noise.

ii. Transimpedence Amplifier Noise

Design of transimpedence amplifier consists of an electronic amplifier with SiFET front end and feedback resistance throughout input-output terminals. Total noise attributable to a transimpedence amplifier is:

a. Thermal noise of feedback resistance, at this stage it is considered as thermal noise,
b. Thermal noise of FET channel resistance, at this stage it is considered as FET noise,
c. FET gate leakage current impulse noise will be considered as FET impulse noise in this stage.

Noise resulting from the influence of temperature and Johnson noise result from an electrical resistance where thermal energy cause random electron flow without applying any voltage. Thermal noise is combined with feedback resistance throughout amplifier terminals. Depending on higher value of the resistance thermal noise current is reduced.

For great bandwidth applications regarding OTDR relatively small feedback resistances which create great thermal noise current are required. This noise is considered as white noise on detection bandwidth. Thermal noise is also combined with channel resistance of FET at the front end of transimpedence amplifier. Contrary to white thermal noise of feedback resistance, thermal noise intensity spectrum of channel resistance changes proportionally to the square of the frequency.

iii. EDFA Noise

Amplified signal and forward amplified spontaneous emission result in the following noise types at receiver:

a. ASE-impulse noise,
b. Signal-ASE impulse noise,
c. ASE-ASE impulse noise.

Similar to signal impulse noise, ASE-impulse noise occurs in photodiodes which appear at the output of EDFA in photodiode and creates random forward ASE. In other words signal ASE noise derives from ASE photons combined with amplified signal spectrum. Classically, it may be considered as the impulse between frequency components of the signal and ASE components in optical signal bandwidth. In other words, signal-ASE impulse noise is uniform in spectral intensity density RF domain.

ASE signal impulse noise therefore cannot be reduced by narrow band filtering method. Consequently this noise exists in nature of optical amplifiers. In other saying, ASE-ASE impulse noise results from impulse signal of frequency components in gain bandwidth of ASE spectrum. This noise can be reduced effectively by using a narrow band optical filter between amplifier output and photo receiver. Intensity spectral density of the noise decreases linear to frequency value at optical bandwidth level [20].

3.7 EDFA / TRANSIMPEDENCE NOISE MODEL

In this model, a noiseless photo diode and an amplifier are considered as sources of noise modeled as current sources throughout amplifier terminals. Here, thermal noise is parallel to the feedback resistance (R_f) and the electrical signal taking input of transimpedence amplifier terminals as reference is deemed as optical bandwidth >> electrical bandwidth. Optical noise figure of an EDFA is indicated as follows.

$$F = \frac{1 + 2n_{sp}(G-1)}{G} \tag{3.5}$$

Electrical signal-noise intensity ratio SNR_e is expressed by the following equation.

$$SNR_e[dB] = 10\log\left[\frac{i^2_{Signal}}{(\sum i_j^2)/N}\right] \tag{3.6}$$

In the equation; N means the average number or signal components processed on the data, j means impulse, various sources such as thermal and FET etc. Furthermore, Optical signal-noise ratio SNR_0 is expressed as follows depending on measured voltage "V":

$$SNR_0[dB] = 20\log\left[\frac{V_{Signal}}{(\sum V_j^{RMS})/\sqrt{N}}\right] \tag{3.7}$$

Voltage value, calculated by a factor of RMS current and feedback resistance, is calculated by using the equation (3.8):

$$V_j = \sqrt{i_j^2}\ R_f \tag{3.8}$$

Another important issue during optical amplification is the possibility of saturation of the receiver by both amplified signal and ASE or other noise sources. Another important issue results in exceeding saturation voltage of the receiver V_{sat} that may cause truncation of required signal.

$$V_{sat} \geq R_f\left(\sqrt{i^2_{pulse}} + \sqrt{i^2_{thermal}} + \sqrt{i^2_{amplifier}} + +.....+ \sqrt{i^2_{Signal}} + I_{ASE}\right) \tag{3.9}$$

ASE is an important problem which causes saturation of the receiver and it can be minimized by using a suitable filtering method.

4. STUDY CONCLUSIONS AND DISCUSSION

4.1 SIMULATION CONDITIONS

A model has been created for the Service Provider system that contains the PON (Passive Optical Network) communication network, in which fiber optic cable is used. In the model, the length of the PON link is taken as 1 km and it is based on single mode optic fiber at 1550 nm for the wavelength in which the attenuation and fiber losses for data transportation are minimum.. The structure given in Figure 4.1 is used as base in the sense of giving you an opinion on the typical appearance of the model used in the simulations.

Figure 4.1: Demonstration of PON service provider used in the model.

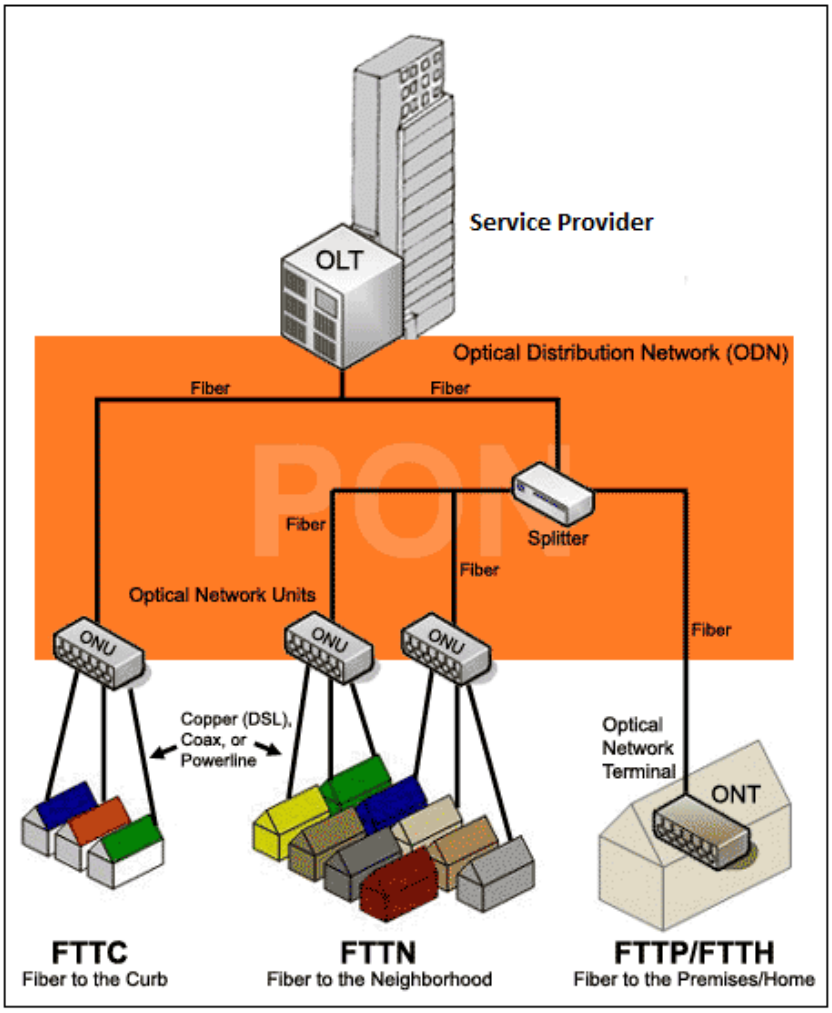

Source: http://ftth.blogsky.com/1391/06/30/post-3/ (14.01.2015)

PON structured service provider used in the model is composed of a OLT (Optical line terminal), three ONU (Optical network unit) structures and two splitters (duplexer-spreader) that ensure communication among these and fiber optic cables connecting units to each other. In the system, communication is ensured by distributing the information coming from the Optical Line Terminal (OLT) to Optical Network Unit 1 (ONU 1) through the splitter and to ONU 2 and ONU 3 through the second splitter.

Making sure that ONU's do not receive the information that does not belong to them from among the information distributed, is one of the most important matters. Other than these, it is assumed that data does not collide as the information from all ONU's will be transmitted to OLT's through a single fiber optic cable after splitter and considered that there is not a signal attenuation that may interrupt data transmission at the receiving party.

In the PON link with the length of 1 km, optic fiber cable from the Optical Line Terminal enters to the first splitter and then to the first Optical Network Unit after a certain distance. After that the same fiber optic cable enters to the second splitter and then the fiber optic cable exiting from the splitter reaches to Optical Network Units respectively.

Simulations related to the Raman power changes of the backscattered signal and heat formations along the cable during the data communication in these PON units for the portion of the fiber optic cable with the length of 1 km, were obtained under the limit conditions and simulation conditions given.

Simulation conditions which were used for obtaining the profile related to Raman power changes and heat formation along the cable and taken as basis for the model, are given below:

1. There is a SPLITTER (first splitter) 200 meters ahead of OLT in the service provider.

2. There is ONU 1 100 meters after the first splitter. While the distance between the Optical Line Terminal (OLT) and ONU 1 is 300 meters, the distance between ONU 1 and the first splitter is 100 meters.

3. The second Splitter is placed 450 meter away from the Optical Line Terminal and 150 meters ahead of ONU 1. The distance between two splitters (between the Splitter 1 and Splitter 2) is 250 meters.

4. There is ONU 2 at the 500TH meter of the optic fiber cable. The distance between ONU and Splitter 2 is only 50 meters.

5. There is ONU 3 at the 780TH meter of the optic fiber cable. ONU 3 is placed 280 away from ONU 2.

6. In the PON service provider model studied, there are total of two Splitter units (Splitter 1 and Splitter 2) and three Optical network units (ONU 1, ONU 2 and ONU 3) for the optic fiber cable with the length of 1 km.

PON link structure used in the model is indicated in Figure 4.2.

Figure 4.2: PON link structure used in the model

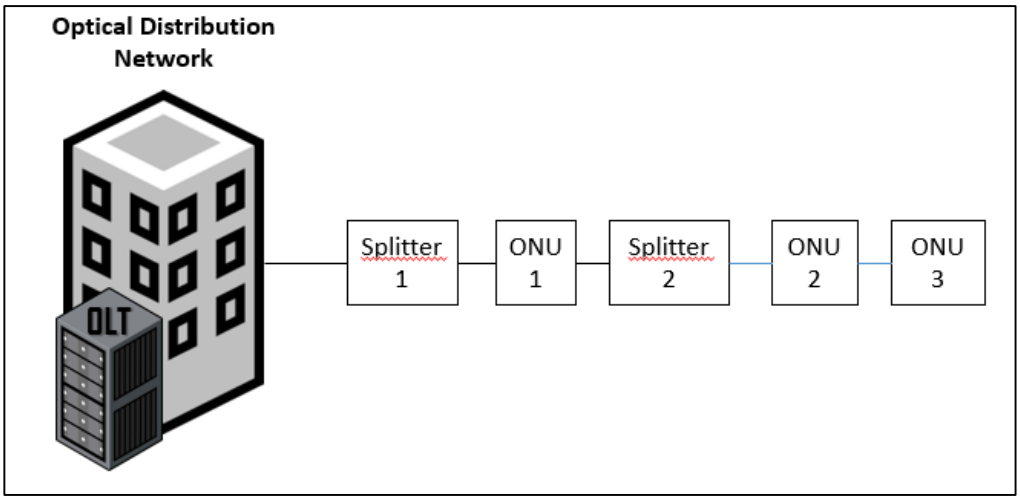

Source: Prepared by Gürkan Kaya

4.2 CALCULATIONS RELATED TO OPTIC FIBER PARAMETERS USED IN SIMULATIONS

In order to obtain temperature data along the cable link for PON link in optic fiber data communication depending on the simulation conditions and on the basis of the criteria given in the selected model, Raman scattering explained in the second section was taken as basis and Raman power changes were exploited. Single mode fiber with 1550 nm wavelength was used in all simulations.

In line with the temperature data, cable temperature formation profile was obtained by making use of the technique basing on Raman and Brillouin scatterings mentioned in the second section. Here; K_{ε}^{P} Brillouin power tension coefficient and K_{T}^{P} Brillouin power temperature coefficients were exploited. Other parameters used in the same were calculated as follows and they were entered to Matlab program according to these results.

Optic fiber parameters used in simulation and calculations related to these parameters:

Fiber length: $L = 1000\ meter$

Pulse duration: 14 ns.

P0: Launched probe power

PB(L): Brillouin power profile along the cable

W: Probe pulse range

VG: Group speed

alpha_B: Brillouin scattering coefficient %1.49e-6;

alpha_R: Rayleigh scattering coefficient

S: Capture fraction (numerically captured scattered light quantity of the optic fiber)

NA: Numerical range of fiber

n: Fiber core-nucleus refraction index
Va: Expresses the speed of acoustic waves occurring in optic fiber based on Raman scattering principle.

p = 0.286; Photo elasticity (Pockel) coefficient.

Ro = 2330; Density of the optical silica, 2330 kg/m3

Va = 5960; Fiber core refraction index 1.5, When optic fiber temperature was taken as 298 degrees Kelvin, VG group speed was taken as 5960 m/s.

Lamda_0 = 1550e-9; percent1550 nm. working wavelength,

alpha_R = 4.68e-5.

P0 = 3; Probe power; 3 Watt

W = 14e-9; Probe pulse width --- 14 ns.

Pulse duration sent into the fiber: $\tau = 14\ ns$.

Spatial Distance (two point resolution), is calculated as:
$\Delta z = \frac{c.\tau}{2n} = \frac{3.10^{8}.x14.10^{-9}}{2x1.5} = 1.4\ m.$

Benefiting from spatial distance expression.

Number of points measured along the cable with spatial distance of 1.4 can be calculated as follows.

$$\frac{Optical\ fiber\ length}{Spatial\ resolution} = \frac{1000}{1.4.} = 714\ points.$$

Therefore, number of measured points= 1 km/1.40 = 714 points used for data reception.

According to Bose-Einstein probability distribution of the photons; Bose-Einstein factor for Stokes lines was calculated from the following equation.

$$\rho_S = \frac{1}{1-\exp(-\Delta E/kT)} = \frac{1}{1-\exp(-50.10^{-3}\,x1.60218.10^{-19}/(1.38054.10^{-23}\,J/K.^{\circ}K(T))} \quad (4.1)$$

Likewise, anti-Stokes lines were calculated from the following formula.

$$\rho_{AS} = \frac{\exp(-\Delta E/kT)}{1-\exp(-\Delta E/kT)} = \frac{\exp(-50.10^{-3}\,x1.60218.10^{-19}/(1.38054.10^{-23}\,J/K.^{\circ}K(T))}{1-\exp(-50.10^{-3}\,x1.60218.10^{-19}/(1.38054.10^{-23}\,J/K.^{\circ}K(T))} \quad (4.2)$$

ρ_S and ρ_{AS} coefficients show change depending on the temperature of the point, where the light is scattered within fiber, in °Kelvin, as seen from the foregoing equations.

In the simulation, Raman-Stokes capture coefficient for 1550 nm in single mode fiber was taken as $\Gamma_{s,\sin gle}(1550nm) = 3.04x10^{-10}$ and $\Gamma_{as,\sin gle}(1550nm) = 4.0x10^{-10}$ and they were entered to Matlab program.

Power attenuation coefficients efficient in Stokes and anti-Stokes waves in 1550 nm for single mode fiber sensor were calculated as;

$$\alpha_{P,S}(dB) = \frac{\alpha_P(\lambda_0) + \alpha_P(\lambda_S)}{2} = \frac{\alpha_P(1550) + \alpha_P(1663)}{2} = \frac{0.20 + 0.22}{2} = 0.21 \quad (4.3)$$

$$\alpha_{P,AS}(dB) = \frac{\alpha_P(\lambda_0) + \alpha_P(\lambda_{AS})}{2} = \frac{\alpha_P(1550) + \alpha_P(1451)}{2} = \frac{0.20 + 0.25}{2} = 0.225 \quad (4.4)$$

Stokes and anti-Stokes coefficients were calculated by using (4.3) and (4.4) equations and $\alpha_{P,S}(neper) = \alpha_{P,S}(dB)x\frac{\ln(10)}{L}$ equation as follows;

$$\alpha_{P,S}(neper) = \alpha_{P,S}(dB)x\frac{\ln(10)}{L} = 0.21x\frac{\ln(10)}{5000} = 9.67x10^{-5} \quad (4.5)$$

$$\alpha_{P,AS}(neper) = \alpha_{P,AS}(dB)x\frac{\ln(10)}{L} = 0.225x\frac{\ln(10)}{5000} = 10.36x10^{-5} = 51.80x10^{-5} \quad (4.6)$$

for the high voltage cable with the length of 1 km.

For PON link with the length of 1 km, the equation given in (4.7) was used in order to obtain Raman power of the back-scattered signal, Rama power along the cable and the temperature profiles for OLT-ONU and optic fiber cable.

$$T(z) = \frac{\Delta E}{k \ln\left[\frac{h_S(t)}{h_{AS}(t)} x \left(\frac{\lambda_S}{\lambda_{AS}}\right)^4 x \exp(\Delta\alpha_P xz)\right]} \quad (4.7)$$

In the equation (4.7) $h_S(t)$ and $h_{AS}(t)$ are Raman power Stokes and Raman power anti-Stokes impulse responses at moment t respectively.

At 1550 nm wavelength, Stoke signal and anti-Stokes signals are reversely guided to light photons inside the optical fiber and back-scattered at 1663 nm and 1451 nm respectively.

4.3 SIMULATION AND ASSESSMENT RELATED TO THE RAMAN POWER OF THE BACK-SCATTERED SIGNAL

Raman power change profile of the back-scattered signal for optic fiber cable with the length of 1 km for PON link for the criteria stated under the simulation conditions is given in Figure 4.3.

Figure 4.3: Raman power change profile for the PON link with the length of 1 km (Percentile change of Raman power along the cable)

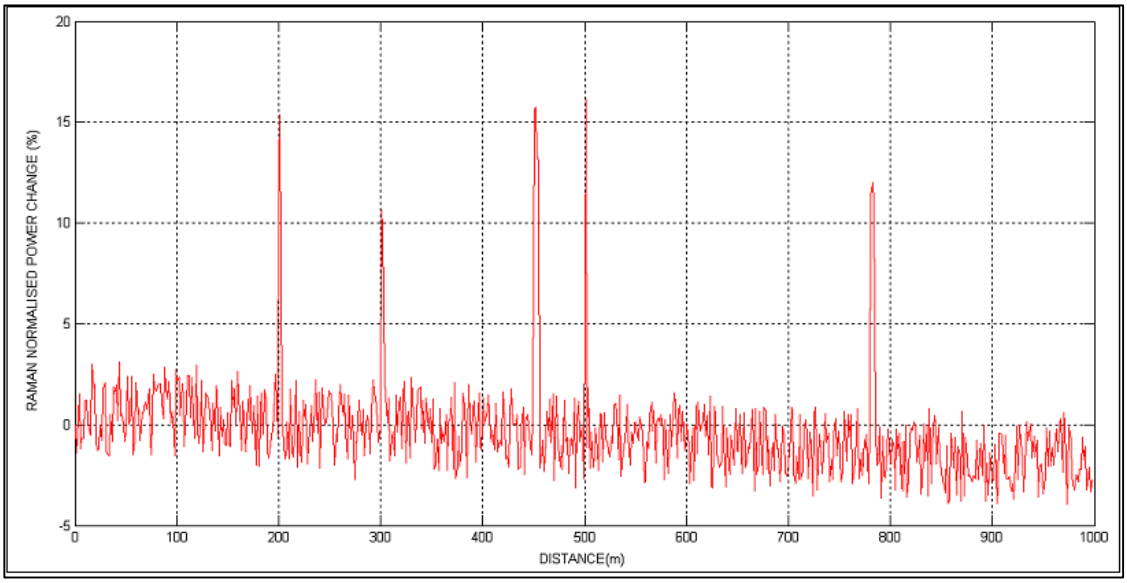

Source: Prepared by Gürkan Kaya

As seen in Figure 4.3, percentile change in the Raman power of the back-scattered signal, reached to its maximum value at the 500TH meter along the cable. Raman power reached its highest value with 15,8 percent at the point where the optic fiber cable reached to Optical network units No.2 (ONU 2) after the second splitter (Splitter 2).

The second region, where the highest Raman power change occurred, was located at the point where the optic fiber entered to the second Splitter. At this point, Raman power reached to the value of 15,5 percent. In Figure 4.4, the point, where the change in the Raman power had reached to is maximum value, was shown.

Figure 4.4: Demonstration of the maximum value of the change in Raman power.

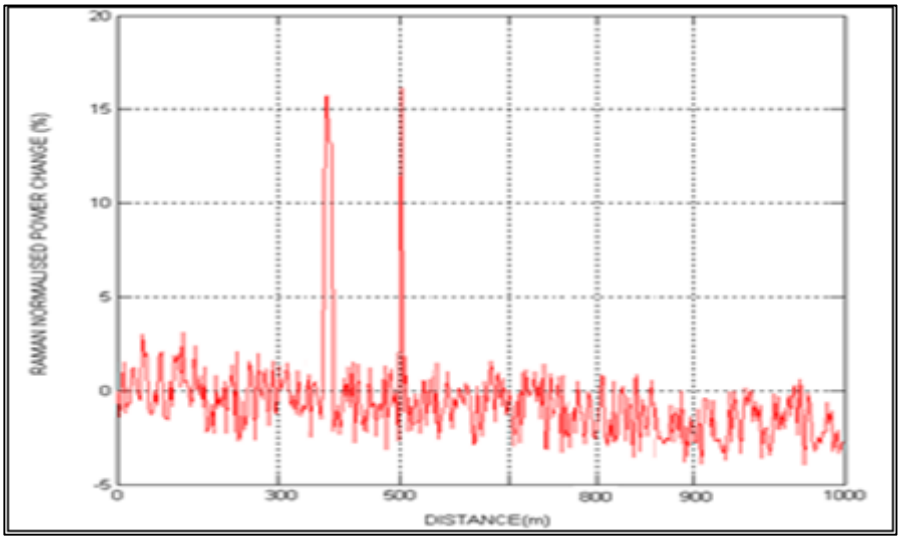

Source: Prepared by Gürkan Kaya

According to the simulation results, at the points along the cable where it entered to ONU 1, ONU 2 and ONU 3, in other words at the 300TH, 500TH and 780TH meters, changes in the Raman power were obtained as 10,4 percent, 15,8 percent and 12,0 percent respectively.

Temperature change profile obtained from Raman power changes along the cable for the PON link with the length of 1 km is given in Figure 4.5 Thermal effects occurring both between the OLT and Splitters and Splitters and ONU's along the optic fiber cable during the data transmission cause back-scattering of light photons advancing through the fiber.

Depending on this phenomenon which was given in detail in the part related to Raman scattering in Section 2, vibrational molecular modes caused by thermal effects in silica material structure of optic fiber (each mode has s structure that advances through the fiber and is explained with electromagnetism theory and Maxwell equations), cause back-scattering of the light photons by interacting with the light photons pumped into the optic fiber.

Based on this non-elastic scattering mechanism which is called the Rama scattering, Raman power changes of the back-scattered optic signal can be obtained.
By using the Raman power changes given in Figure 4.3 and expression given in equation (4.7), it is possible to obtain temperature change profile along the cable length given for PON link model.

Temperature changes profile obtained for back-scattered signal in OLT-Splitter and ONU line in the optic fiber cable structure with the length of 1 km under the simulation conditions are given in Figure 4.6.

As it is obvious from the graph, there is a linear change in the temperature formations occurring along the cable depending on the change in Raman power. However, the temperature increase at the point where the optic fiber cable joins with Splitter 2, was higher when compared to the linear increase in Raman power changes at such point.

At this point, where the temperature change was the highest and the optic fiber cable enters to Splitter 2 along the PON link, temperature change occurred was 46.8 °C.

Temperature change at the point where the optic fiber cable enters to Splitter 2 is shown in Figure 4.5.

Figure 4.5: Temperature change in Splitter 2 is demonstrated

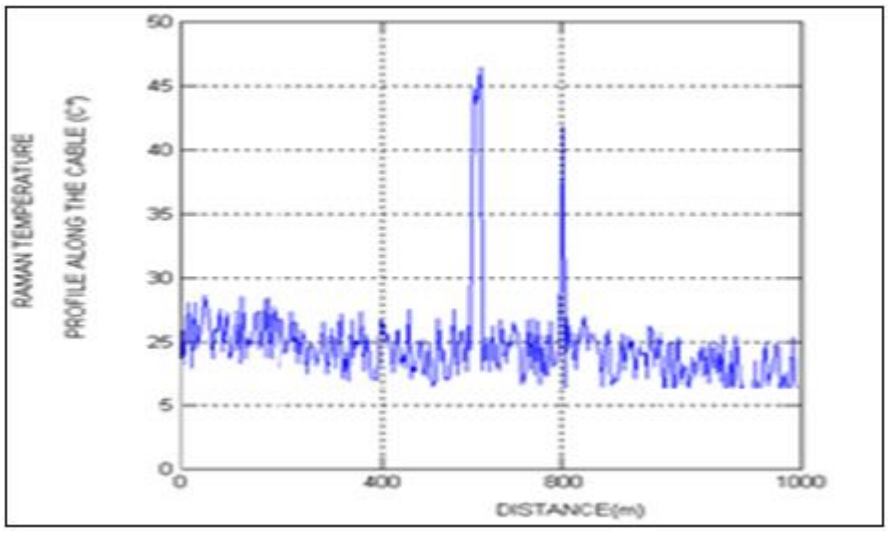

Source: Prepared by Gürkan Kaya

Temperature changes along the cable reached to ~ 44.2 °C at Splitter 1, 200 meters away from OLT. Temperature changes obtained in ONU 1, ONU 2 and ONU 3 were 40.8 °C, 42.0 °C and 41.7 °C respectively. Temperature increase occurred at ONU 1, in other words, at the 300TH meter on the cable, was lower when compared to other cable joint or system entry points.

Figure 4.6: Temperature change profile of Raman power in back-scattered Signal along the PON link with the length of 1 km

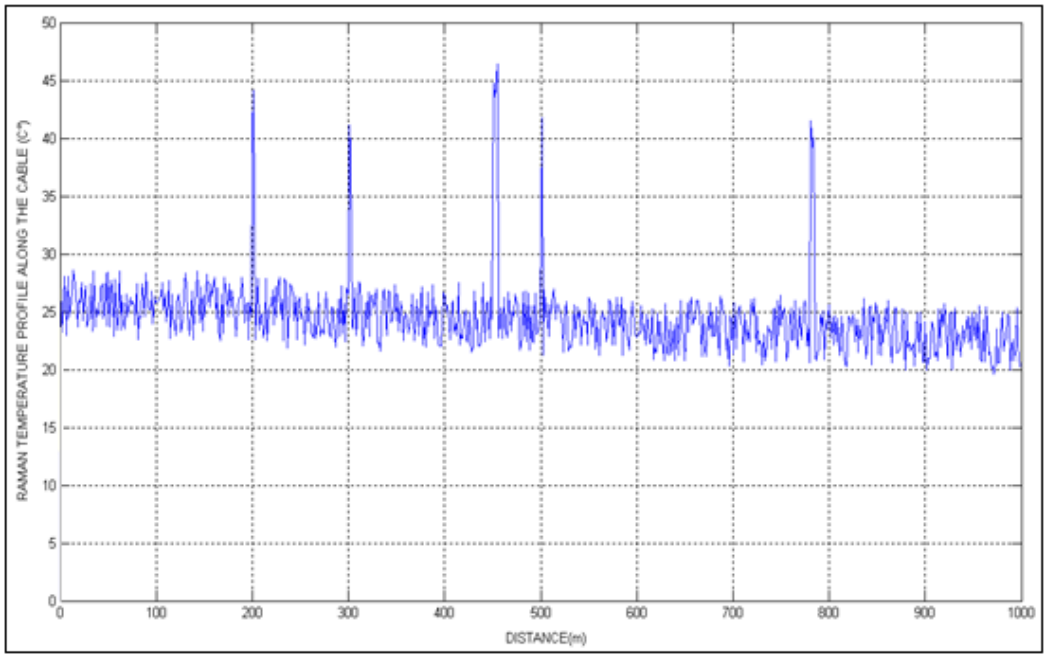

Source: Prepared by Gürkan Kaya

As is seen, the areas with the highest temperature increases along the fiber cable, appeared as points where the cable entered to the Splitters.

While the changes in Raman power reached the highest value on PON system at ONU 2, observing the temperature increase in Splitter 2 happened due to the fact that Splitters have an electronic design that cause higher temperature generation when compared to ONU's.

5. CONCLUSIONS

In this thesis, use of Passive Optical Networks (PON) in data communication in optic fiber communication has been examined and comprehensive information has been given about passive optical networks by mentioning about PON types. Furthermore, details about signal attenuation and optic fiber losses have been also added.

Moreover in this study, backwards scattering mechanisms of the optic signal in optic fiber data cable have been emphasized for a selected PON model, Raman power changes of the signal and temperature formations along the cable have been simulated and assessed by using Matlab program.

The region, where the highest Raman power change occurred, was located at the point where the optic fiber enters to the second Splitter. At this point, Raman power reached to the value of 15,5 percent.

According to the simulation conditions, changes and increases have been observed in terms of both Raman power and temperature formations at ONU 1, ONU 2 and ONU 2 parts along the cable.

In the light of this data, change in the Raman power of the optical signal can be determined while working on PON link or previously and therefore errors and problems that may occur in data transmission (due to both temperature and attenuation) can be determined in advance.

In other words, it is important to the detect the temperature formation which is an important factor and/or effect that decreases the life of the optic fiber cable and hot points caused by the thermal effects occurring on the cable insulation and take measures before they cause adverse effects.

Thus this study may be useful in terms of having an opinion on temperature formations in advance and taking precautions before facing with data loss by the final user.

REFERENCES

[1] YILMAZ, G. KARLIK, S.E. A real-time temperature monitoring application on high voltage cables with optical fiber sensors. Proceedings of the Ninth National Congress of Electrical-Electronics and Computer Engineering, 30-34p. İzmit, Turkey, 2001.

[2] Robert W. Keyes, "The Impact of Moore's Law", IEEE Solid-State Circuits, September, 2006.

[3] Gail Robinson, "Architects of the Internet: David Bishop", EE Times, Sept. 26, 2000.

[4] D.van den Borne, V.A.J.M. Sleiffer, M.S.Alfiad, S.L. Jensen, and T. Wuth, "POLMEX-QPSK Modulation and Coherent Detection: the Challenge of Long-Haul 100G Transmission", Proc. European Conference on Optical Communications, paper 3.4.1, 2009.

[5] http://bilisimdergi.com

[6] Turna Ö., Aydin M.A., Zaim A.H., "Pasif Optik Erişim Ağlarının Gelişimi" Akademik Bilişim'09, XI. Akademik Bilişim Konferansı Bildirileri, Şanlıurfa, 2009.

[7] Agrawal, G. P., Fiber-Optic Communication Systems, A John Wiley & Sons, INC., Publication, 2002.

[8] http://grouper.ieee.org/groups/802/3

[9] http://www.fsanweb.org/nga.asp

[10] Hornung, S. Davey, R., Payne, D., Nesset, D. , "Evolution to next generation optical access Networks", Lasers and Electro-Optics Society,. The 20th Annual Meeting of the IEEE, 21-25 Oct. 2007

[11] Koonen A. M. J. , "Fiber to the Home/Fiber to the Premises: What,Where, and When?" Proceedings of the IEEE, vol. 94, no. 5, pp. 911–934, May 2006.

[12] http://www.ciscotr.com/forum/qos-quality-service/3460-quality-serviceqos-nedir-quality-service-qos-konfigurasyonu-nasil-yapilir-qos-nedir.html

[13] D.R.T. Jorgesen "Improved Techniques for Passive Optical Networks", Doktora Tezi, University Of California, San Diego, 2010.

[14] WDM-PON Technologies, www.ciphotonics.com/download/whitepaper WPON_ White_Paper_v10.pdf

[15] H. Ishio, J. Minowa, and K. Nosu, "Review and Status of Wavelength-Division-Multiplexing Technology and Its Application", J.Light. Tech., vol. LT-2, no. 4, pp. 448-463, 1984.

[16] J. Bromage, P.J. Winzer, and R-J. Essiambre, "Multiple Path Interference and Its Impact on System Design" in Raman Amplifiers for Telecommunications 2, M.N. Islam, Ed. New York: Springer-Verlag, ch. 15, 2004.

[17] K.Rasmus, M.Tafur, O.Leif, J.Palle "Impairments Due to Burst-Mode Transmission in a Raman-Based Long-Reach PON Link" IEEE Photonics Technology Letter, Vol. 19, No. 19, October, 2007.

[18] N.J. Frigo, P.P. Iannone, P.D. Magill, T.E. Darcie, M.M. Downs, B.N. Desai, U. Koren, T.L. Koch, C. Dragone, H.M. Presby, and G.E. Bodeep, "A Wavelength-Division Multiplexed Passive Optical Network with Cost-Shared Components", IEEE Phot. Tech. Lett., vol. 6, no. 11, pp. 1365-1367, 1994.

[19] K.Rasmus, M.Tafur, O.Leif, J.Palle "Distributed fiber Raman amplification in long reach PON bidirectional access links", Optical Fiber Technology 14 (2008) 41–44

[20] Günday A. "Enerji Kablosunda Oluşan Sıcaklık ve Gerilmeleri Optik Fiberli Algılayıcılarla Algılama Benzetimleri", Yüksek Lisans Tezi, Uludağ Üniversitesi Fen Bilimleri Enstitüsü, Bursa, 2007.

[21] ALAHBABİ M.N. "Distributed optical fiber sensors based on the Coherent detection of Spontaneous Brillouin Scattering", PhD Thesis, 2005.

[22] J. Wilson and J. Hawkes, Optoelectronics and Introduction, 3rd ed. Prentice Hall, 1998.

[23] Kurashima, M.Tateda, T.Horiguchi, and Y.Koyamada, "Performance improvement of a combined OTDR for distributed strain and loss measurement by randomizing the reference light polarization state," IEEE Photon, Technol. Lett., vol. 9, 360 (1997).

[24] Analog Haberleşme, Kayran A. Birsen Yayınevi, 2002.

APPENDICES

Appendix-1 Change of Raman and Raman Power Gain Power Simulation Program / Matlab 7.0.

```
clear

% Figure(1)

% Set(1,'Name','1km uzunluğundaki FTTH PON Linkinde OLT--ONU arasında
RAMAN GUCU DEGERLENDIRME--RAMAN GUCU degisimi')

% 1550nm dalga boyunda Basamak indisli Tek modlu Fiber
Kullanılmaktadır.


% 1: OLT den 200 metre ileride bir SPLITTER (BÖLÜCÜ) ve 2. ONU dan
sonra 1 SPLITTER daha bulunmaktadır (450.metrede)bulunmaktadır.

% 2: SPLITTER den sonra 3 adet ONU fiber kablo ile beslenmektedir.
%    ONU lar sırasıyla;

300. metrede,
500. metrede,
780. metrede yer almaktadır. Her birinde sıcaklık artışları
olmaktadır.

% Uzamsal Aralık (iki nokta çözünürlüğü)
% R : Ölçüm alınan nokta sayısı = 1 km/1.40 = 714 ayrı noktadan veri
alımı yapılmıştır.

% Darbe süresi:14ns.

% P0: Launched probe power

% PB(L): Kablo boyunca Brillouin güç profili

% W: Probe darbe genişliği

% VG: Grup hız

% alpha_B: Brillouin saçılma katsayısı %1.49e-6; nüve kırılma indisi
1.5, fiber sıcaklıgı 298 Kelvin, VG grup hızı 5960 m/s. olarak
alınmıstır.

% alpha_R: Rayleigh saçılma katsayısı

% S: Capture fraction (optik fiberin nümerik açıklığında yakalanan
saçılmış ışık miktarı)

% NA: Fiberin nümerik açıklığı
```

```
% n: Fiber çekirdek-nüve kırılma indisi

% p: Foto elastike (Pockel) katsayısı (0.286)

% Va: Akustik hız

p = 0.286;

Ro = 2330;  %2330 silikanın yoğunluğu kg/m3

Va = 5960;  %5960 m/s

Lamda_0 = 1550e-9; %1550 nm. çalışma dalga boyu

% alpha_R = 4.68e-5;

P0 = 3; % Probe gücü; 1 Watt

W = 14e-9; % Probe darbe genişliği 120 mWatt-14 ns.

% Kablo boyunca benzetimde kullanılan kablo üzerindeki noktalar

% Uzamsal Aralık (iki nokta çözünürlüğü)

% R : Ölçüm alınan nokta sayısı = 1 km /1.4 = 714 adet

% Darbe süresi:15ns.

L = 1000;       % Fiber Kablonun Uzunluğu (metre)

Delta_z=1.4;    % Metre cinsinden uzamsal aralık
Delta_z=14*e-9*3*e8/(2*1.5) Formülünden çıkartılmıştır.

Kappa_s = 3.04e-10;  (1550nm dalga boyunda tek modlu fiber için)

Kappa_as = 4.0e-10;  (1550nm dalga boyunda tek modlu fiber için)

Alpha_ps = 9.67e-5;    Alpha_ps = (adb*1n(10)/5000)= 9.67e-5 olarak
bulunur.

Alpha_pas = 10.36e-5; % Alpha_pas = 10.36e-5 olarak bulunur.

R=715;

d=rand(R,1)-0.5;

cc1=rand(R,1)-0.5;

for m=2:R-1;

z(m)=(m-1)*1.4;

S = (1.4^2-1.38^2)/(4*(1.4^2));
```

```
% S = 0.004975(yandaki işlem yerine direk olarak ta konabilir, NA;
n1=1.5 ve n2=1.485 e göre hesaplandı)
% NA = karekök (n1 kare - n2 kare) ifadesinden hesaplanmıştır.

Va = 5960;

Vg = (3e8)/1.4;

% s=((ro_s*Kappa_s+d(m)*1e-12)*(1-exp(-2*Alpha_ps*3e8*15e-9*(m)/3)))
/((ro_as*Kappa_as+cc1(m)*1e-12)*(1-exp(-2*Alpha_pas*3e8*15e-
9*(m)/3)));

% 5 km uzunluğundaki Yüksek Gerilim Kablosu üzerinde Raman ve
Brillouin % saçılmaları baz alınarak Dağınık Sıcaklığın hesaplatılması

if z(m) >= 200 & z(m) <= 202

%BRILLOUIN GÜÇ

S = (1.5^2-1.48^2)/(4*(1.5^2));
alpha_B = (8*(3.1415926)^3*(1.5)^8*(0.286)^2*1.38e-
23*312)/(3*(Lamda_0)^4*Ro*(Va)^2);

alpha_R = (8*(3.1415926)^3*(1.5)^8*(0.286)^2*1.38e-23*1950)*(7e-11-
1/(Ro*(Va)^2))/(3*(Lamda_0)^4);

PB(m)=0.5*P0*W*alpha_B*S*Vg*exp(-2*alpha_R*z(m)+2.1)*1e8/4+d(m)*0.2-8;
T(m)=25 + PB(m)/0.36;

%RAMAN GÜÇ

ro_s=1/(1-exp((-0.05*1.60218e-19)/(1.38054e-23*312)));

%Delta_E=Ramanda (E2--E1) moleküler enerji düzeyleri arasındaki
farktır. Delta_E=hV(6.62e-34*13.5 THz.) formülünden bulunmaktadır.

ro_as=exp((-0.05*1.60218e-19)/(1.38054e-23*312))/(1-exp((-
0.05*1.60218e-19)/ (1.38054e-23*312)));

s(m)=((ro_s*Kappa_s+d(m)*1e-12*3)*(1-exp(-2*Alpha_ps*3e8*15e-9*z(m))))
/((ro_as*Kappa_as+cc1(m)*1e-12*3)*(1-exp(-2*Alpha_pas*3e8*15e-
9*z(m))));

TR(m)= 25 + 50e-3*1.60218e-19/(1.38054e-
23*log(s(m)*(1663/1451)^4*exp(1.3e-6*z(m))))-264;

PR(m)= 0.8*(TR(m)-25);

elseif  z(m) >= 300 & z(m) <= 303

S = (1.5^2-1.48^2)/(4*(1.5^2));

alpha_B = (8*(3.1415926)^3*(1.5)^8*(0.286)^2*1.38e-
23*310)/(3*(Lamda_0)^4*Ro*(Va)^2);
```

```
alpha_R = (8*(3.1415926)^3*(1.5)^8*(0.286)^2*1.38e-23*1950)*(7e-11-
1/(Ro*(Va)^2))/(3*(Lamda_0)^4);

PB(m)=0.5*P0*W*alpha_B*S*Vg*exp(-2*alpha_R*z(m)+2.1)*1e8/4+d(m)*0.2-8;

T(m)=25 + PB(m)/0.36;

%RAMAN GÜÇ

ro_s=1/(1-exp((-0.05*1.60218e-19)/(1.38054e-23*310)));

%Delta_E=Ramanda (E2--E1) moleküler enerji düzeyleri arasındaki
farktır. Delta_E=hV(6.62e-34*13.5 THz.) formülünden bulunmaktadır.

ro_as=exp((-0.05*1.60218e-19)/(1.38054e-23*310))/(1-exp((-
0.05*1.60218e-19)/ (1.38054e-23*310)));

s(m)=((ro_s*Kappa_s+d(m)*1e-12*3)*(1-exp(-2*Alpha_ps*3e8*15e-9*z(m))))
/((ro_as*Kappa_as+cc1(m)*1e-12*3)*(1-exp(-2*Alpha_pas*3e8*15e-
9*z(m))));

TR(m)= 25 + 50e-3*1.60218e-19/(1.38054e-
23*log(s(m)*(1663/1451)^4*exp(1.3e-6*z(m))))-264;

PR(m)= 0.8*(TR(m)-25);

elseif  z(m) >= 450 & z(m) <= 455

S = (1.5^2-1.48^2)/(4*(1.5^2));

alpha_B = (8*(3.1415926)^3*(1.5)^8*(0.286)^2*1.38e-
23*316)/(3*(Lamda_0)^4*Ro*(Va)^2);

alpha_R = (8*(3.1415926)^3*(1.5)^8*(0.286)^2*1.38e-23*1950)*(7e-11-
1/(Ro*(Va)^2))/(3*(Lamda_0)^4);

PB(m)=0.5*P0*W*alpha_B*S*Vg*exp(-2*alpha_R*z(m)+2.1)*1e8/4+d(m)*0.2-8;

T(m)=25 + PB(m)/0.36;

%RAMAN GÜÇ

ro_s=1/(1-exp((-0.05*1.60218e-19)/(1.38054e-23*316)));

%Delta_E=Ramanda (E2--E1) moleküler enerji düzeyleri arasındaki
farktır. Delta_E=hV(6.62e-34*13.5 THz.) formülünden bulunmaktadır.
ro_as=exp((-0.05*1.60218e-19)/(1.38054e-23*316))/(1-exp((-
0.05*1.60218e-19)/ (1.38054e-23*316)));

s(m)=((ro_s*Kappa_s+d(m)*1e-12*3)*(1-exp(-2*Alpha_ps*3e8*15e-9*z(m))))
/((ro_as*Kappa_as+cc1(m)*1e-12*3)*(1-exp(-2*Alpha_pas*3e8*15e-
9*z(m))));

TR(m)= 25 + 50e-3*1.60218e-19/(1.38054e-
23*log(s(m)*(1663/1451)^4*exp(1.3e-6*z(m))))-264;
```

```
PR(m)= 0.8*(TR(m)-25);

elseif  z(m) >= 500 & z(m) <= 502

S = (1.5^2-1.48^2)/(4*(1.5^2));
alpha_B = (8*(3.1415926)^3*(1.5)^8*(0.286)^2*1.38e-
23*317)/(3*(Lamda_0)^4*Ro*(Va)^2);

alpha_R = (8*(3.1415926)^3*(1.5)^8*(0.286)^2*1.38e-23*1950)*(7e-11-
1/(Ro*(Va)^2))/(3*(Lamda_0)^4);

PB(m)=0.5*P0*W*alpha_B*S*Vg*exp(-2*alpha_R*z(m)+2.1)*1e8/4+d(m)*0.2-8;

T(m)=25 + PB(m)/0.36;

%RAMAN GÜÇ

ro_s=1/(1-exp((-0.05*1.60218e-19)/(1.38054e-23*317)));

%Delta_E=Ramanda (E2--E1) moleküler enerji düzeyleri arasındaki
farktır. Delta_E=hV(6.62e-34*13.5 THz.) formülünden bulunmaktadır.

ro_as=exp((-0.05*1.60218e-19)/(1.38054e-23*317))/(1-exp((-
0.05*1.60218e-19)/ (1.38054e-23*317)));

s(m)=((ro_s*Kappa_s+d(m)*1e-12*3)*(1-exp(-2*Alpha_ps*3e8*15e-9*z(m))))
/((ro_as*Kappa_as+cc1(m)*1e-12*3)*(1-exp(-2*Alpha_pas*3e8*15e-
9*z(m))));

TR(m)= 25 + 50e-3*1.60218e-19/(1.38054e-
23*log(s(m)*(1663/1451)^4*exp(1.3e-6*z(m))))-264;

PR(m)= 0.8*(TR(m)-25);

elseif  z(m) >= z(m) >= 640 & z(m) <= 646

S = (1.5^2-1.48^2)/(4*(1.5^2));

alpha_B = (8*(3.1415926)^3*(1.5)^8*(0.286)^2*1.38e-
23*308)/(3*(Lamda_0)^4*Ro*(Va)^2);

alpha_R = (8*(3.1415926)^3*(1.5)^8*(0.286)^2*1.38e-23*1950)*(7e-11-
1/(Ro*(Va)^2))/(3*(Lamda_0)^4);

PB(m)=0.5*P0*W*alpha_B*S*Vg*exp(-2*alpha_R*z(m)+2.1)*1e8/4+d(m)*0.2-8;

T(m)=25 + PB(m)/0.36;


%RAMAN GÜÇ

ro_s=1/(1-exp((-0.05*1.60218e-19)/(1.38054e-23*308)));

%Delta_E=Ramanda (E2--E1) moleküler enerji düzeyleri arasındaki
farktır. Delta_E=hV(6.62e-34*13.5 THz.) formülünden bulunmaktadır.
```

```
ro_as=exp((-0.05*1.60218e-19)/(1.38054e-23*308))/(1-exp((-
0.05*1.60218e-19)/ (1.38054e-23*308)));

s(m)=((ro_s*Kappa_s+d(m)*1e-12*3)*(1-exp(-2*Alpha_ps*3e8*15e-9*z(m))))
/((ro_as*Kappa_as+cc1(m)*1e-12*3)*(1-exp(-2*Alpha_pas*3e8*15e-
9*z(m))));

TR(m)= 25 + 50e-3*1.60218e-19/(1.38054e-
23*log(s(m)*(1663/1451)^4*exp(1.3e-6*z(m))))-264;

PR(m)= 0.8*(TR(m)-25);

elseif  z(m) >= 780 & z(m) <= 784

S = (1.5^2-1.48^2)/(4*(1.5^2));

alpha_B = (8*(3.1415926)^3*(1.5)^8*(0.286)^2*1.38e-
23*314)/(3*(Lamda_0)^4*Ro*(Va)^2);

alpha_R = (8*(3.1415926)^3*(1.5)^8*(0.286)^2*1.38e-23*1950)*(7e-11-
1/(Ro*(Va)^2))/(3*(Lamda_0)^4);

PB(m)=0.5*P0*W*alpha_B*S*Vg*exp(-2*alpha_R*z(m)+2.1)*1e8/4+d(m)*0.2-8;

T(m)=25 + PB(m)/0.36;

%RAMAN GÜÇ

ro_s=1/(1-exp((-0.05*1.60218e-19)/(1.38054e-23*314)));

%Delta_E=Ramanda (E2--E1) moleküler enerji düzeyleri arasındaki
farktır. Delta_E=hV(6.62e-34*13.5 THz.) formülünden bulunmaktadır.

ro_as=exp((-0.05*1.60218e-19)/(1.38054e-23*314))/(1-exp((-
0.05*1.60218e-19)/ (1.38054e-23*314)));

s(m)=((ro_s*Kappa_s+d(m)*1e-12*3)*(1-exp(-2*Alpha_ps*3e8*15e-9*z(m))))
/((ro_as*Kappa_as+cc1(m)*1e-12*3)*(1-exp(-2*Alpha_pas*3e8*15e-
9*z(m))));

TR(m)= 25 + 50e-3*1.60218e-19/(1.38054e-
23*log(s(m)*(1663/1451)^4*exp(1.3e-6*z(m))))-264;

PR(m)= 0.8*(TR(m)-25);


elseif  z(m) >= 920 & z(m) <= 921

S = (1.5^2-1.48^2)/(4*(1.5^2));

alpha_B = (8*(3.1415926)^3*(1.5)^8*(0.286)^2*1.38e-
23*324)/(3*(Lamda_0)^4*Ro*(Va)^2);

alpha_R = (8*(3.1415926)^3*(1.5)^8*(0.286)^2*1.38e-23*1950)*(7e-11-
1/(Ro*(Va)^2))/(3*(Lamda_0)^4);
```

```
PB(m)=0.5*P0*W*alpha_B*S*Vg*exp(-2*alpha_R*z(m)+2.1)*1e8/4+d(m)*0.2-8;

T(m)=25 + PB(m)/0.36;

%RAMAN GÜÇ

ro_s=1/(1-exp((-0.05*1.60218e-19)/(1.38054e-23*324)));

%Delta_E=Ramanda (E2--E1) moleküler enerji düzeyleri arasındaki
farktır. Delta_E=hV(6.62e-34*13.5 THz.) formülünden bulunmaktadır.

ro_as=exp((-0.05*1.60218e-19)/(1.38054e-23*324))/(1-exp((-
0.05*1.60218e-19)/ (1.38054e-23*324)));

s(m)=((ro_s*Kappa_s+d(m)*1e-12*3)*(1-exp(-2*Alpha_ps*3e8*15e-9*z(m))))
/((ro_as*Kappa_as+cc1(m)*1e-12*3)*(1-exp(-2*Alpha_pas*3e8*15e-
9*z(m))));

PR(m)= 0.8*(TR(m)-25);

else

S = (1.5^2-1.48^2)/(4*(1.5^2));
alpha_B = (8*(3.1415926)^3*(1.5)^8*(0.286)^2*1.38e-
23*300)/(3*(Lamda_0)^4*Ro*(Va)^2);

alpha_R = (8*(3.1415926)^3*(1.5)^8*(0.286)^2*1.38e-23*1950)*(7e-11-
1/(Ro*(Va)^2))/(3*(Lamda_0)^4);

%RAMAN GÜÇ

ro_s=1/(1-exp((-0.05*1.60218e-19)/(1.38054e-23*300)));

%Delta_E=Ramanda (E2--E1) moleküler enerji düzeyleri arasındaki
farktır. Delta_E=hV(6.62e-34*13.5 THz.) formülünden bulunmaktadır.

ro_as=exp((-0.05*1.60218e-19)/(1.38054e-23*293))/(1-exp((-
0.05*1.60218e-19)/ (1.38054e-23*293)));

s(m)=((ro_s*Kappa_s+d(m)*1e-12*3)*(1-exp(-2*Alpha_ps*3e8*15e-9*z(m))))
/((ro_as*Kappa_as+cc1(m)*1e-12*3)*(1-exp(-2*Alpha_pas*3e8*15e-
9*z(m))));

TR(m)= 25 + 50e-3*1.60218e-19/(1.38054e-
23*log(s(m)*(1663/1451)^4*exp(1.3e-6*z(m))))-264;

PR(m)= 0.8*(TR(m)-25);

% PB güç ifadesini NORMALİZE etmek için kullanılmaktadır. SIFIR olarak
ta alınabilir.


end
%-------------------------------------------------------------------
---------------------------------
```

```
end

subplot(221)
plot(z,PB,'r-')

grid on

xlabel('DISTANCE(m)'); ylabel('BRILLOUIN NORMALISED POWER CHANGE (%)')

subplot(222)

plot (z,T,'b-')

grid on

xlabel('DISTANCE(m)'); ylabel('BRILLOUIN TEMPERATURE PROFILE ALONG THE
CABLE (C°)')

subplot(223)

plot(z,PR,'r-')

grid on

xlabel('DISTANCE(m)'); ylabel('RAMAN NORMALISED POWER CHANGE (%)')

subplot(224)

plot (z,TR,'b-')

grid on

xlabel('DISTANCE(m)'); ylabel('RAMAN TEMPERATURE PROFILE ALONG THE
CABLE (C°)')
figure(2)

plot(z,PR,'r-')

grid on

xlabel('DISTANCE(m)'); ylabel('RAMAN NORMALISED POWER CHANGE (%)')

figure(3)

plot (z,TR,'b-')

grid on

xlabel('DISTANCE(m)'); ylabel('RAMAN TEMPERATURE PROFILE ALONG THE
CABLE (C°)')

figure(4)

plot(TR+273,PR,'r-')

grid on

xlabel('DISTANCE(m)'); ylabel('RAMAN NORMALISED POWER CHANGE (%)')
```